The Black-Scholes and Heston Models for Option Pricing

by

Ziqun Ye

A thesis
presented to the University of Waterloo
in fulfillment of the
thesis requirement for the degree of
Master of Mathematics
in
Statistics

Waterloo, Ontario, Canada, 2013

I hereby declare that I am the sole author of this thesis. This is a true copy of the thesis, including any required final revisions, as accepted by my examiners.

I understand that my thesis may be made electronically available to the public.

Abstract

Stochastic volatility models on option pricing have received much study following the discovery of the non-at implied surface following the crash of the stock markets in 1987. The most widely used stochastic volatility model is introduced by Heston (1993) because of its ability to generate volatility satisfying the market observations, being non-negative and mean-reverting, and also providing a closed-form solution for the European options. However, little research has been done on Heston model used to price early-exercise options. This presumably is largely due to the absence of a closed-form solution and the increase in computational requirement that complicates the required calibration exercise. This thesis examines the performance of the Heston model versus the Black-Scholes model for the American Style equity option of Microsoft and the index option of S&P 100 index. We employ a finite difference method combined with a Projected Successive Over-relaxation method for pricing an American put option under the Black-Scholes model, while an Alternating Direction Implicit method is utilized to decompose a multi-dimensional partial differential equation into several one dimensional steps under the Heston model. For the calibration of the Heston model, we apply a two step procedure where in the first step we apply an indirect inference method to historical stock prices to estimate diffusion parameters under a probability measure and then use a least squares method to estimate the instantaneous volatility V_t and the market risk premium λ which are used to switch from working under the probability measure to working under the risk-neutral measure.

We find that option price is positively related with the value of the mean reverting speed, κ and the long-term variance, θ. It is not sensitive to the market price of risk, λ; and it is negatively related with the risk free rate, r and the volatility of volatility, σ. By comparing the European put option and the American put option under the Heston model, we observe that their implied volatility generally follow similar patterns. However, there are still some interesting observations that can be made from the comparison of the two put options. First, for the out-of-the-money category, the American and European options have rather comparable implied volatilities with the American options' implied volatility being slightly bigger than the European options. While for the in-the-money category, the implied volatility of the European options is notably higher than the American options and its value exceeds the implied volatility of the American options.

We also assess the performance of the Heston model by comparing its result with the result from the Black-Scholes model. We observe that overall the Heston model performs better than the Black-Scholes model. In particular, the Heston model has tendency of underpricing the in-the-money option and overpricing the out-of-the-money option. Whereas,

the Black-Scholes model is inclined to underprice both the in-the-money option and the out-of-the-money option.

Acknowledgements

I would like to express my sincere thanks and gratitude to my supervisor, Prof. Tony S. Wirjanto, for his patient guidance and valuable advice he has provided though my whole research period. Thanks to Prof. Wirjanto, I insisted in writing this thesis and gradually build up my research skills. I thank him for his prompt response to my emails every time and both academic and financial support.

Also, I would like to thank Prof. Chengguo Weng. Prof. Weng has provided valuable suggestions in Chapter 4 for the calculating the implied volatility.

Dedication

This is dedicated to my parents and my friend Wuyang Zhang and Fei Meng. Without their help and encouragement, I can not finish this thesis on time.

Table of Contents

List of Tables

List of Figures

Chapter 1

Introduction

In the past decades or so, various stochastic volatility (SV) models for option pricing have been introduced to capture the volatility smile effect, among which the Heston Model has been given most prominence due to its ability to produce volatility smile, being non-negative and mean-reverting, and also provide a closed-form solution for European options. Comparatively, however, little research has been done on applying Heston Model to early-exercise options, probably due to the fact that a closed-form solution for the price is not available and that an additional computational requirement for the model relative to the standard Black-Scholes (1973) [2] raises the complexity involved in the calibration. This has hampered further the use of pricing models in the option markets which provides a motivation for this thesis.

Previously, most studies have been conducted to price the European option by an Alternating Direction Implicit method [24], while little has been done on the American options. In this thesis, we employ an Alternating Direction Implicit method to the Heston model to provide an efficient solution for not only the European options but also the American Option. For pricing under the Black-Scholes model, a finite difference method combined with a Projected Successive Over-Relaxation method [27] is utilized.

After discussing how to price the American option and the European option under both the Heston model and the Black-Scholes model, we work on the calibration for both models. Fiorentini G., Leoń A. and Rubio G. (2002) [7] introduce a two-step estimation method. In the first step, an indirect inference method is used to estimate the structural parameters in the Heston model which affect the asset return distribution. The core idea is to match the stock price series generated from the Heston Model and the series generated from an estimated Nonlinear Asymmetric Generalized AutoRegressive Conditional

1

Heteroskedasticity(NAGARCH) [6] model from the historical stock prices; the second step is to estimate the value of risk premium and the instantaneous variance by minimizing the distance between the market prices and the model prices using the least squares method.

We are going to explore the relationship between the option price and the diffusion parameters. Then, implied volatility of the American option and European option under the two models will be presented to assess the implications of how both models perform. The real market data such as Microsoft options and S&P 100 index options are used for assessment of the performance of this extended Heston model (1993) [16] by comparing it with the result from the Black-Scholes model. It is found that overall the Heston model performs better than the Black-Scholes model. However, the Heston model has a tendency to undervalue the in-the-money option and overprice the out-of-the-money option. Whereas, the Black-Scholes model is inclined to underprice both the in-the-money option and the out-of-the-money option.

The rest of the thesis is organized as follows. Chapter 2 introduces the Black-Scholes model and the method to evaluate the European style option and the American style option under the Black-Scholes model. Then, it discusses the method of the calibration of the Black-Scholes model. We also discuss its limitations at the end of Chapter 2. Chapter 3 presents the Heston model and also studies how to price both the European style option and the American style option. Then, the calibration of the Heston model is presented. In Chapter 4, we implement a series of numerical tests. Firstly, we apply the Heston model to the American option. Then, we explore the performance of the Heston model in generating the implied volatility. Lastly, we calibrate the Heston model on an Equity option and an index option and analyze its performance. Chapter 5 gives the conclusion.

Chapter 2

Black-Scholes Model and Option Pricing

2.1   Notation

$S(t)$ is the stock price at time t where $S_0 = S(0)$ is the current stock price.

$C(S,t)$ is the theoretical European call option price which is a function of stock price $S(t)$ and t.

T is the maturity time.

K is the strike price.

r is the short term interest rate

σ is the standard deviation of the stock return

2.2   Assumptions for the Black-Scholes Equation

(a) The short-term interest rate is known and constant for all maturities.

(b) The volatility of the stock return is constant over time. The logarithm of the stock price follows a Brownian Motion. Thus the distribution of the stock prices is lognormal which is equivalent to saying that the continuously compounded return of stock is normally distributed: $d \ln S_t \sim N\left((r - \sigma^2/2)dt, \sigma^2 dt\right)$

(c) There is no dividend paid during the life of the option.

(d) The option is European style, which can only be exercised at the expiration date.

(e) There are no transaction costs, margins or taxes.

(f) It is possible to short-sell any amount of stock and to borrow any amount of money at the short-term interest rate.

2.3   Black-Scholes Model

Under Black-Schole model, it is assumed that the stock price obeys the following stochastic process:
$$dS_t = \mu S_t dt + \sigma S_t dW_t \tag{2.1}$$
where μ is the drift term, σ is the standard deviation of the stock returns and W_t is a standard Brownian motion. Black-Scholes (1973) shows that we can use the risk-neutral probability rather than the true probability to evaluate the price of an option, as long as we discount it at the risk-free rate instead of the true rate. It is due to the fact that under such a measure discounted price processes are martingales, which guarantees no arbitrage. In the risk-neutral world, we have

$$dS_t = r S_t dt + \sigma S_t dW_t \tag{2.2}$$

2.4   Derivation of Partial Differential Equation (PDE) from the Black-Scholes Model

Suppose that we buy one share of stock, then we need to short $1/\frac{\partial C(S,t)}{\partial S}$ number of call option to avoid a loss at the maturity T due to a decrease in stock price. To see why we need to buy $1/\frac{\partial C(S,t)}{\partial S}$ number of option, let us assume that the stock price changes by dS, then the option price will change by $\frac{\partial C(S,t)}{\partial S} \cdot dS$ where $\frac{\partial C(S,t)}{\partial S}$ is the ratio of a change in the option price due to the dS change in the stock price. Therefore, we lose dS from holding one share of the stock and earn $1/\frac{\partial C(S,t)}{\partial S} \cdot \frac{\partial C(S,t)}{\partial S} \cdot dS = dS$. In total, the hedged position does not change due to the change in the stock price.

The value of the position at time t is

$$S_t - \frac{C(S,t)}{\frac{\partial C(S,t)}{\partial S}}. \tag{2.3}$$

At time dt, the stock price changes by dS. The value of the change in the position at time t is

$$dS - \frac{(C(S+dS,t+dt) - C(S,t))}{\frac{\partial C(S,t)}{\partial S}}. \tag{2.4}$$

Ito's lemma for Brownian motion is:

$$df(W_t,t) = \partial_\omega f(W_t,t)dW_t + \frac{1}{2}\partial_\omega^2 f(W_t,t)dt + \partial_t f(W_t,t)dt \tag{2.5}$$

By using the Ito's lemma (2.5), we can write the following expression:

$$C(S+dS,t+dt) - C(S,t) = \frac{\partial C(S,t)}{\partial S}dS + 0.5\frac{\partial^2 C(S,t)}{\partial S^2}\sigma^2 S^2 dt + \frac{\partial C(S,t)}{\partial t}dt. \tag{2.6}$$

Plug (2.6) into (2.4), we obtain the change in the position as:

$$-\left(\frac{1}{2}\frac{\partial^2 C(S,t)}{\partial S^2}\sigma^2 S^2 + \frac{\partial C(S,t)}{\partial t}\right)dt \cdot \frac{1}{\frac{\partial C(S,t)}{\partial t}} \tag{2.7}$$

If we keep hedging the position continuously, the position will have no risk over time. Hence, we will earn a profit at the risk free interest rate r over time. Therefore,

$$-\left(\frac{1}{2}\frac{\partial^2 C(S,t)}{\partial S^2}\sigma^2 S^2 + \frac{\partial C(S,t)}{\partial t}\right)dt \cdot \frac{1}{\frac{\partial C(S,t)}{\partial S}} = \left(S_t - \frac{C(S,t)}{\frac{\partial C(S,t)}{\partial S}}\right)rdt \tag{2.8}$$

After rearrangement of terms, we get:

$$\frac{\partial C(S,t)}{\partial t} = rC(S,t) - rS\frac{\partial C(S,t)}{\partial S} - \frac{1}{2}\sigma^2 S^2\frac{\partial^2 C(S,t)}{\partial S^2} \tag{2.9}$$

It is demonstrated that the value of any asset must satisfy standard arbitrage argument. More generally, any derivatives with an underlying stock follow the same stochastic process would

The payoff of the European Call Option is

$$C(S,T) = S(T) - K, \qquad\qquad S(T) \geq K \qquad\qquad (2.10)$$
$$= 0, \qquad\qquad S(T) < K$$

2.4.1 European Call Option Price

The call option price satisfies the PDE (2.9) and the boundary condition. The final solution is:

$$C(S,t) = SN(d_1) - Ke^{r(t-T)}N(d_2)$$
$$d_1 = \frac{\ln S/K + (r + \frac{1}{2}\sigma^2)(T-t)}{v\sqrt{T-t}} \qquad\qquad (2.11)$$
$$d_2 = \frac{\ln S/K + (r - \frac{1}{2}\sigma^2)(T-t)}{v\sqrt{T-t}}$$

2.4.2 Another Way to Derive the Call Option Price

In section 2.3, we mentioned that Black-Scholes assumes the risk-neutrality. Since in the risk-neutral world all assets earn the risk-free rate, the continuously compounded rate of return of the stock price $\alpha = \ln(S_{t+1}/S_t)$ is normally distributed with its expected value being equal to $(r - \frac{1}{2}\sigma^2)T$. The probability that $S_T > K$ is therefore given by $N(d_2)$, where d_2 is evaluated using the risk-free rate. $N(d_1)$ is the risk-neutral expectation proportion of S_T/S_0, given that $S_T > K$, where expectation proportion of a random variable over a range is the partial expectation conditional on that range divided by the total expectation. We can derive the option price formula in another way shown below as $\frac{S_T}{S_0} \sim lognormal(\mu T, \sigma^2 T)$ where $\mu = r - 0.5\sigma^2$

$$\mathrm{E}[max(0, S_T - K)]$$
$$= \ \mathrm{E}[max(S_T - K, 0)|S_T \geq K]P(S_T \geq K) + \mathrm{E}[max(S_T - K, 0)|S_T < K]P(S_T < K)$$
$$= \ \mathrm{E}[S_T - K|S_T \geq K]P(S_T \geq K) + E[0|S_T < K]P(S_T < K)$$
$$= \ \mathrm{E}[S_T|S_T \geq K]P(S_T \geq K) + KP(S_T \geq K) + 0$$
$$= \ \frac{S_0 e^{rT} N(d_1)}{N(d_2)} N(d_2) + KN(d_2)$$
$$= \ S_0 e^{rT} N(d_1) + KN(d_2)$$

For a European call option, we need to discount it to current time to arrive at its price.
$C(S_0, K, 0, T) = e^{-rt} \mathrm{E}[max(0, S_T - K)] = S_0 N(d_1) + Ke^{-rT} N(d_2)$, where $\frac{S_0 e^{rT} N(d_1)}{N(d_2)}$ represents the future value of the underlying asset conditional on the stock price at maturity being greater than the strike price K.

$$\mathrm{E}[S_T|S_T > K] = S_0 E \left[\frac{S_T}{S_0} | \frac{S_T}{S_0} > \frac{K}{S_0} \right]$$
$$= \ S_0 \frac{1}{N(d_2)} \int_{\frac{K}{S_0}}^{\infty} \frac{x e^{-(\ln x - \mu T)^2 / 2\sigma^2 T dx}}{x \sigma \sqrt{2\pi T}} dx$$
$$= \ S_0 \frac{1}{N(d_2)} \int_{\frac{K}{S_0}}^{\infty} \frac{e^{-(\ln x - \mu T)^2 / 2\sigma^2 T dx}}{\sigma \sqrt{2\pi T}} dx$$

Let $y = \ln x - \mu T$, then we have $x = e^{y + \mu T}$. Take an infinitesimally small difference on both sides and we have $dx = e^{y + \mu T} dy$. Substitute this into (2.12) to yield,

$$\frac{1}{N(d_2)} \frac{1}{\sigma \sqrt{2\pi T}} \int_{\ln \frac{K}{S_0} - \mu T}^{\infty} e^{-y^2 / 2\sigma^2 T} e^{y + \mu T} dy$$

$$= \frac{1}{N(d_2)} \frac{e^{\mu T}}{\sigma \sqrt{2\pi T}} \int_{\ln \frac{K}{S_0} - \mu T}^{\infty} e^{(-y^2 - 2\sigma^2 T y) / 2\sigma^2 T} dy$$

$$= \frac{1}{N(d_2)} e^{\mu T + 0.5\sigma^2 T} \int_{\ln \frac{K}{S_0} - \mu T}^{\infty} \frac{1}{\sigma \sqrt{2\pi T}} e^{-(y - \sigma^2 T)^2 / 2\sigma^2 T} dy$$

$$= \frac{1}{N(d_2)} e^{\mu T + 0.5\sigma^2 T} \left[1 - N \left(\frac{\ln \frac{K}{S_0} - \mu T - \sigma^2 T}{\sigma \sqrt{T}} \right) \right]$$

$$= \frac{1}{N(d_2)} \mathrm{E}[X] N \left(-\frac{\ln \frac{K}{S_0} - \mu T - \sigma^2 T}{\sigma \sqrt{T}} \right)$$

$$= \frac{1}{N(d_2)} \mathrm{E}[X] N \left(\frac{\ln \frac{S_0}{K} + rT + 0.5\sigma^2 T - \sigma^2 T}{\sigma \sqrt{T}} \right)$$

$$= \frac{1}{N(d_2)} \mathrm{E}[X] N \left(\frac{\ln \frac{S_0}{K} + rT - 0.5\sigma^2 T}{\sigma \sqrt{T}} \right)$$

$$= \frac{\mathrm{E}[X] N(d_1)}{N(d_2)}$$

2.5   American Option

There are two basic types of a call option to consider: European option and American option. A European option can only be exercised at maturity while an American option can be exercised before or at expiration.

2.5.1   Comparison of European Option and American Option

The most obvious difference between the American option and the European option is that an American option can be exercised at or before the expiration date while a European Option can be only exercised at expiration. This entails at least a no smaller value of American options than an otherwise similar European option. Generally the American

option is of the same value as the European option as the time premium associated with the remaining life of an option makes early exercise sub-optimal. In spite of this, there are two exceptions: one is when the value of the underlying asset is largely decreased by large dividends. A possible exercise can take place right before the dividend payment date where the time value on the options is less than the expected reduction in the asset value. The other is when an investor holds both the underlying asset and deep in-the-money puts on that asset with a high interest rate. The profit gained from exercising the put early and from interest on the exercise price can exceed the time value on the put.

2.6   Black-Scholes Model for American options

In this thesis, we only focus on pricing non-dividend options. Previously in section 2.4.1 and section 2.4.2, we have discussed how to evaluate a European call option. The European put option price can be obtained through the put-call parity. Due to the fact that the American call option with no dividend is of the same value with the European one, we are more interested in pricing the American put option in this thesis. All the methods being used to price an American option are presented by Wilmott, P., Howison, S., Dewynne, J. [27].

Let $V(S,t)$ be the price of an American put option. We mentioned in section 2.5 that American option can be early exercised, and therefore, its payoff should be at least as big as that of an otherwise identical European put option:

$$V(S,t) \geq (E - S, 0) \tag{2.12}$$

Also, the price of an American put option satisfies the Black-Schole inequality:

$$\frac{\partial V(S,t)}{\partial t} + rS\frac{\partial V(S,t)}{\partial S} + \frac{1}{2}\sigma^2 S^2 \frac{\partial^2 V(S,t)}{\partial S^2} - rV(S,t) \leq 0 \tag{2.13}$$

2.6.1   The Black-Scholes Formula

In order to simplify the computation of American put options price, we need to transform the Black-Scholes equation (2.9) into the famous heat equation form [1]:

$$\frac{\partial^2 y}{\partial x^2} = \frac{\partial y}{\partial \tau} \tag{2.14}$$

with $y(x,\tau)$, $x \in \mathbb{R}$, $\tau \geq 0$.

Instead of dealing with the Black-Schole inequality, for simplicity let us for this moment focus on a European put option with a value of $P(S,t)$ which satisfies the Black-Scholes equation:

$$\frac{\partial P(S,t)}{\partial t} + rS\frac{\partial P(S,t)}{\partial S} + \frac{1}{2}\sigma^2 S^2 \frac{\partial^2 P(S,t)}{\partial S^2} - rP(S,t) = 0 \tag{2.15}$$

The following shows how Wilmott, P., Howison, S., Dewynne, J. [27] transform the Black-scholes equation into the diffusion equation.

Let $S = Ke^x$, $t = T - \tau/\frac{1}{2}\sigma^2$, $P = Kv(x,\tau)$.

Substitute this into equation (2.15) we get

$$\frac{dv}{d\tau} = \frac{d^2 v}{dx^2} + (k-1)\frac{dv}{dx} - kv$$

where $k = \tau/(\frac{1}{2}\sigma^2)$. The initial condition for a European put option becomes

$$v(x,0) = \max(1 - e^x, 0).$$

Further, let us put $v = e^{\alpha x + \beta \tau} u(x,\tau)$ for some constants α and β to be determined, and differentiation gives

$$\beta u + \frac{du}{d\tau} = \alpha^2 u + 2\alpha\frac{du}{dx} + \frac{d^2 u}{dx^2} + (k-1)(\alpha u + \frac{du}{dx}) - ku.$$

We can obtain an equation with no u term by choosing

$$\beta = \alpha^2 + (k-1)\alpha - k$$

---

[1] A partial differential equation the solution of which gives the distribution of temperature in a region as a function of space and time when the temperature at the boundaries, the initial distribution of temperature, and the physical properties of the medium are specified.

while the choice $0 = 2\alpha + (k - 1)$ eliminates the $\frac{du}{dx}$ term as well. These equations for α and β give $\alpha = -\frac{1}{2}(k - 1)$, and $\beta = -\frac{1}{4}(k + 1)^2$. We then have

$$v = e^{-\frac{1}{2}(k-1)x - \frac{1}{4}(k+1)^2\tau} u(x, \tau), \tag{2.16}$$

where

$$\frac{du}{d\tau} = \frac{d^2u}{dx^2} \qquad \text{for} -\infty < x < \infty, \ \tau > 0,$$

with $u(x, 0) = u_0(x) = max(e^{\frac{1}{2}(k-1)x} - e^{\frac{1}{2}(k+1)x}, 0)$

Now let us go back to the American put option problem. The possibility of early exercise raises a free boundary problem. Howison, S., Dewynne, J. and Wilmott, P. [27] choose to reduce the free boundary problem to a fixed boundary one by transforming it into the linear complementarity form.

Let the transformed payoff constraint function $g(x, \tau)$ be:

$$g(x, \tau) = e^{\frac{1}{4}(k+1)^2\tau} \max(e^{\frac{1}{2}(k-1)x} - e^{\frac{1}{2}(k+1)x}, 0) \tag{2.17}$$

Then, the American valuable problem can be written into the following compact linear complementarity form:

$$\left(\frac{\partial u}{\partial \tau} - \frac{\partial^2 u}{\partial x^2}\right) \geq 0, \quad (u(x, \tau) - g(x, \tau)) \geq 0, \tag{2.18}$$

$$\left(\frac{\partial u}{\partial \tau} - \frac{\partial^2 u}{\partial x^2}\right) \cdot \left(u(x, \tau) - g(x, \tau)\right) = 0$$

with the initial condition:

$$u(x, 0) = g(x, 0) \tag{2.19}$$

2.6.2   Finite-difference Approximations

After transforming the Black-Scholes Formula into a diffusion equation, we next show how to solve the diffusion equation numerically. A finite-difference method [27] approximates the partial derivatives by Taylor series expansions. There are mainly three types of approximation depending on the directions of the parameters: forward difference, backward difference, and central difference methods. Take the partial derivative of $du/d\tau$ as an

11

example. The forward difference is defined as

$$\frac{du}{d\tau}(x,\tau) = \lim_{\delta\tau \to 0} \frac{u(x, \tau + \delta\tau) - u(x, \tau)}{\delta\tau}$$

We can also write it in another way by assuming that $\delta\tau$ infinitesimally small but nonzero, then we obtain the following result:

$$\frac{du}{d\tau}(x,\tau) \approx \frac{u(x, \tau + \delta\tau) - u(x, \tau)}{\delta\tau} + O(\delta\tau) \tag{2.20}$$

Similarly, the backward difference is defined as:

$$\frac{du}{d\tau}(x,\tau) = \lim_{\delta\tau \to 0} \frac{u(x, \tau) - u(x, \tau - \delta\tau)}{\delta\tau}$$

so that the approximation is of the form:

$$\frac{du}{d\tau}(x,\tau) \approx \frac{u(x, \tau) - u(x, \tau - \delta\tau)}{\delta\tau} + O(\delta\tau) \tag{2.21}$$

Likewise, we define central differences to be:

$$\frac{du}{d\tau}(x,\tau) = \lim_{\delta\tau \to 0} \frac{u(x, \tau + \delta\tau) - u(x, \tau - \delta\tau)}{2\delta\tau}$$

This gives rise to the following approximation:

$$\frac{du}{d\tau}(x,\tau) \approx \frac{u(x, \tau + \delta\tau) - u(x, \tau - \delta\tau)}{2\delta\tau} + O((\delta\tau)^2) \tag{2.22}$$

We will deal with the partial derivatives of x in exactly the same manner.

$$\frac{du}{dx}(x,\tau) \approx \frac{u(x + \delta x, \tau) - u(x - \delta x, \tau)}{2\delta x} + O((\delta x)^2) \tag{2.23}$$

For the second order derivative, we can define it by taking the central difference between the forward difference of the first derivative and the backward difference of the second

derivative as follows:

$$\frac{d^2u}{dx^2}(x,\tau) \approx \frac{\frac{u(x+\delta x,\tau)-u(x,\tau)}{\delta x} - \frac{u(x,\tau)-u(x-\delta x,\tau)}{\delta x}}{\delta x} + O((\delta x)^2)$$

$$\frac{d^2u}{dx^2}(x,\tau) \approx \frac{u(x+\delta x,\tau)-2u(x,\tau)+u(x-\delta x,\tau)}{(\delta x)^2} + O((\delta x)^2) \qquad (2.24)$$

We approximate the mixed derivative term by:

$$\frac{d^2u}{dxd\tau} = \frac{\frac{u(x+\delta x,\tau+\delta\tau)-u(x-\delta x,\tau+\delta\tau)}{2\delta x} - \frac{u(x+\delta x,\tau-\delta\tau)-u(x-\delta x,\tau-\delta\tau)}{2\delta x}}{2\delta\tau}$$

$$\frac{d^2u}{dxd\tau} = \frac{u(x+\delta x,\tau+\delta\tau)-u(x-\delta x,\tau+\delta\tau)-u(x+\delta x,\tau-\delta\tau)+u(x-\delta x,\tau-\delta\tau)}{4\delta x\delta\tau} \qquad (2.25)$$

2.6.3 Implicit Finite-difference Method

In the implicit finite-difference method [27], we employ a backward-difference method to approximate the $du/d\tau$ term and symmetric central-difference method to approximate d^2u/dx^2 term. This gives rise to the following equation:

$$\frac{u_n^m - u_n^{m-1}}{\delta\tau} + O(\delta\tau) = \frac{u_{n+1}^m - 2_n^m + u_{n-1}^m}{(\delta x)^2} + O((\delta x)^2),$$

If we ignore the $O(\delta\tau)$ and $O((\delta x)^2)$ terms, we can get

$$-\alpha u_n^m + (1+2\alpha)u_n^m - \alpha u_n^{m+1} = u_n^{m-1}. \qquad (2.26)$$

where $\alpha = \frac{\delta\tau}{(\delta x)^2}$. In the implicit finite-difference method in equation (2.26), u_n^m, u_{n-1}^m and u_{n+1}^m all depend on u_n^{m-1} in an implicit manner. We can write equation (2.26) conveniently as a linear system

$$\begin{pmatrix} 1+2\alpha & -\alpha & 0 & ... & 0 \\ -\alpha & 1+2\alpha & -\alpha & & 0 \\ 0 & -\alpha & \ddots & \ddots & \\ \vdots & & \ddots & \ddots & -\alpha \\ 0 & 0 & & -\alpha & 1+2\alpha \end{pmatrix} \begin{pmatrix} u_{N^-+1}^m \\ \vdots \\ u_0^m \\ \vdots \\ u_{N^+-1}^m \end{pmatrix} = \begin{pmatrix} u_{N^-+1}^{m-1} \\ \vdots \\ u_0^{m-1} \\ \vdots \\ u_{N^+-1}^{m-1} \end{pmatrix} + \alpha \begin{pmatrix} u_{N^-}^m \\ 0 \\ \vdots \\ 0 \\ u_{N^+}^m \end{pmatrix} = \begin{pmatrix} b_{N^-+1}^m \\ \vdots \\ b_0^m \\ \vdots \\ b_{N^+-1}^m \end{pmatrix}$$

$$(2.27)$$

13

Then we can write equation (2.27) in more compactly as:

$$Mu^m = b^m \tag{2.28}$$

where u^m and b^m denote a $(N^+ - N^- - 1)-$ dimensional vector

$$u^m = (u^m_{N^-+1}, \ldots, u^m_{N^+-1}), \quad b^m = u^{m-1} + \alpha(u^m_{N^-}, 0, \ldots, 0, u^m_{N^+})$$

and M is a $(N^+ - N^- - 1)-$dimensional square symmetric matrix given in (2.27).

2.6.4   The Successive Over-Relaxation Method

The Successive Over-Relaxation (SOR) method [27] is used to solve the equation system (2.27) iteratively. It originates from a Gauss-Seidel method which is a refinement of the Jacobi method.

In order to understand the SOR method well, let us discuss the Jacobi method first. Let us rearrange the terms in the equation system (2.26) in the form

$$u^m_n = \frac{1}{1+2\alpha}(b^m_n + \alpha(u^m_{n-1} + u^m_{n+1})), \ N^- + 1 \le n \le N^+ - 1 \tag{2.29}$$

For the Jacobi method, we first give an initial guess say $u^{m,0}_n$. Then we iteratively solve the following equation:

$$u^{m,k+1}_n = \frac{1}{1+2\alpha}(b^m_n + \alpha(u^{m,k}_{n-1} + u^{m,k}_{n+1})), \ N^- + 1 \le n \le N^+ - 1 \tag{2.30}$$

until the error between $u^{m,k+1}$ and $u^{m,k}$

$$\|u^{m,k+1} - u^{m,k}\|^2 = \sum_n (u^{m,k+1}_n - u^{m,k}_n)^2$$

becomes sufficiently small. The Gaussian-Seidel (GS) method is a refinement of the Jacobi method. It uses the updated $u^{m,k+1}_{n-1}$ immediately instead of $u^{m,k}_{n-1}$.

$$u^{m,k+1}_n = \frac{1}{1+2\alpha}(b^m_n + \alpha(u^{m,k+1}_{n-1} + u^{m,k}_{n+1})), \ N^- \le n \le N^+ \tag{2.31}$$

The SOR is a further development of GS Method by applying extrapolation to the GS method, which is actually a weighted average between the previous iteration and the

14

computed GS iteration successively for each component:

$$u_n^{m,k+1} = \omega y_n^{m,k+1} \tag{2.32}$$

$$y_n^{m,k+1} = \frac{1}{1+2\alpha}(b_n^m + \alpha(u_{n-1}^{m,k+1} + u_{n+1}^{m,k})), \ N^- \leq n \leq N^+ \tag{2.33}$$

$$u_n^{m,k+1} = u_n^{m,k} + \omega(y_n^{m,k+1} - u_n^{m,k}) \tag{2.34}$$

2.6.5 The Crank-Nicolson Method

Crank-Nicolson finite-difference method [27] converges faster at a speed of $O((\delta\tau)^2)$. Essentially the Crank-Nicolson implicit finite scheme is an average of the implicit and explicit methods.

$$\frac{u_n^{m+1} - u_n^m}{\delta\tau} + \frac{u_n^{m+1} - u_n^m}{\delta\tau} + O(\delta\tau) = \frac{u_{n+1}^m - 2u_n^m + u_{n-1}^m}{(\delta x)^2} + \frac{u_{n+1}^{m+1} - 2u_n^{m+1} + u_{n-1}^{m+1}}{(\delta x)^2} + O((\delta x)^2).$$

Let us rearrange the terms in the above equation to yield:

$$\frac{u_n^{m+1} - u_n^m}{\delta\tau} + O(\delta\tau) = \frac{1}{2}\left(\frac{u_{n+1}^m - 2u_n^m + u_{n-1}^m}{(\delta x)^2} + \frac{u_{n+1}^{m+1} - 2u_n^{m+1} + u_{n-1}^{m+1}}{(\delta x)^2}\right) + O((\delta x)^2) \tag{2.35}$$

where as before, we set $\alpha = \delta\tau/(\delta x)^2$.

Unlike the explicit finite-difference method, the Crank-Nicolson finite-difference method does not need any stability and convergence restrictions.

2.6.6 Finite-difference Formulation

Now let us apply the finite difference method to the linear complementarity equations (2.18). We divide the (x, τ)-plane into meshes by step sizes of $\delta\tau$ and δx and set x between $N^-\delta x$ and $N^+\delta x$:

$$N^-\delta x \leq n\delta x \leq N^+\delta x.$$

Howison S. Dewynne J. Wilmott, P. [27] used the Crank-Nicolson scheme to approximate the terms $\frac{\partial u}{\partial \tau}$ and $\frac{\partial^2 u}{\partial x^2}$. We denote the discretized payoff as:

$$g_n^m = g(n\delta x, m\delta\tau) \tag{2.36}$$

We end up with:

$$u_n^{m+1} - \frac{1}{2}\alpha(u_{n+1}^{m+1} - 2u_n^{m+1} + u_{n-1}^{m+1}) \geq u_n^m + \frac{1}{2}\alpha(u_{n+1}^m - 2u_n^m + u_{n-1}^m),$$

$$u_n^m \geq g_n^m \quad \text{for m} \geq 1$$

$$((1+\alpha)u_n^{m+1} - \frac{1}{2}\alpha(u_{n+1}^{m+1} + u_{n-1}^{m+1}) - Z_n^m)(u_n^{m+1} - g_n^{m+1}) = 0 \tag{2.37}$$

where α is defined the same as before (2.26), Z_n^m is defined as:

$$Z_n^m = (1-\alpha)u_n^m + \frac{1}{2}\alpha(u_{n+1}^m + u_{n-1}^m).$$

Let us rewrite the linear complimentary problem (2.37) in a matrix form:

$$Cu^{m+1} \geq b^m \tag{2.38}$$
$$u^{m+1} \geq g^{m+1} \tag{2.39}$$
$$(u^{m+1} - g^{m+1}) \cdot (Cu^{m+1} - b^m) = 0. \tag{2.40}$$

where

$$C = \begin{pmatrix} 1+\alpha & -\frac{1}{2}\alpha & 0 & ... & 0 \\ -\frac{1}{2}\alpha & 1+\alpha & -\frac{1}{2}\alpha & & 0 \\ 0 & -\frac{1}{2}\alpha & \ddots & \ddots & \\ \vdots & & \ddots & 1+\alpha & -\frac{1}{2}\alpha \\ 0 & 0 & & -\frac{1}{2}\alpha & 1+\alpha \end{pmatrix} \tag{2.41}$$

$$u^m = \begin{pmatrix} u_{N^-+1}^m \\ \vdots \\ u_0^m \\ \vdots \\ u_{N^+-1}^m \end{pmatrix}, \quad g^m = \begin{pmatrix} g_{N^-+1}^m \\ \vdots \\ g_0^m \\ \vdots \\ g_{N^+-1}^m \end{pmatrix} \tag{2.42}$$

$$b^m = \begin{pmatrix} b_{N^-+1}^m \\ \vdots \\ b_0^m \\ \vdots \\ b_{N^+-1}^m \end{pmatrix} = \begin{pmatrix} Z_{N^-+1}^m \\ \vdots \\ Z_0^m \\ \vdots \\ Z_{N^+-1}^m \end{pmatrix} + \frac{1}{2}\alpha \begin{pmatrix} g_{N^-}^{m+1} \\ 0 \\ \vdots \\ 0 \\ g_{N^+}^{m+1} \end{pmatrix} \tag{2.43}$$

16

2.6.7 Projected Successive Over-Relaxation (PSOR) Method

Next we use the Projected SOR (PSOR) algorithm to solve for (2.38). PSOR is an adapted version of the SOR algorithm described in section 2.6.4. Apply the SOR algorithm first to a Crank-Nicolson finite difference formulation of the linear complementary problem, we obtain:

$$y_n^{m+1,k+1} = \frac{1}{1+\alpha}(b_n^m + \alpha(u_{n-1}^{m+1,k+1} + u_{n+1}^{m+1,k})), \ N^- \leq n \leq N^+ \tag{2.44}$$

$$u_n^{m+1,k+1} = u_n^{m+1,k} + \omega(y_n^{m+1,k+1} - u_n^{m+1,k}) \tag{2.45}$$

We require $u^{m+1} \geq g^{m+1}$ in our problem. Hence, the second equation is modified as:

$$u_n^{m+1,k+1} = max(u_n^{m+1,k} + \omega(y_n^{m+1,k+1} - u_n^{m+1,k}), g_n^{m+1}) \tag{2.46}$$

Thus, we do the iteration until the difference $||u^{m+1,k+1} - u^{m+1,k}||$ is small enough and then set $u^{m+1} = u^{m+1,k+1}$.

2.7 Calibration of the Black-Scholes Model

In section 2.3 we introduce the the stochastic process (2.1). Let $x_t = ln(S_t)$ and apply Ito's Lemma to (2.1) to obtain:

$$dx_t = (r - \sigma^2/2)dt + \sigma dW_t \tag{2.47}$$

where the unknown parameters is σ. There are two ways of estimating volatility:

- *Historical volatility*: According to Gross, P [23], given $n + 1$ historical prices, calculate $x_i = \ln(\frac{S_i}{S_{i-1}})$ for all t and the historical volatility $\hat{\sigma}$ is an unbiased estimate of the standard deviation of x_i, that is $\hat{\sigma} = \frac{\sqrt{\frac{1}{n-1}\sum_{i=1}^{n}(x_i-\bar{x})^2}}{\sqrt{\tau}}$ where $\bar{x}$ is the sample average of all x_i, S_i is the stock price in period i, and τ is the total length of each period in years.

- *Implied volatility*: Start with the market option price and back out σ from the market option price using the Black-Scholes model.

In this thesis, we use the implied volatility measure.

2.8 Limitations of the Black-Scholes Model

2.8.1 Normal Distribution

Black-Scholes formula is known to have bias in pricing the option because of the assumption that continuously compounded stock returns are normally distributed with known constant mean and variance. An example of S&P 100 is shown here to explain why normal distribution assumption does not work well.
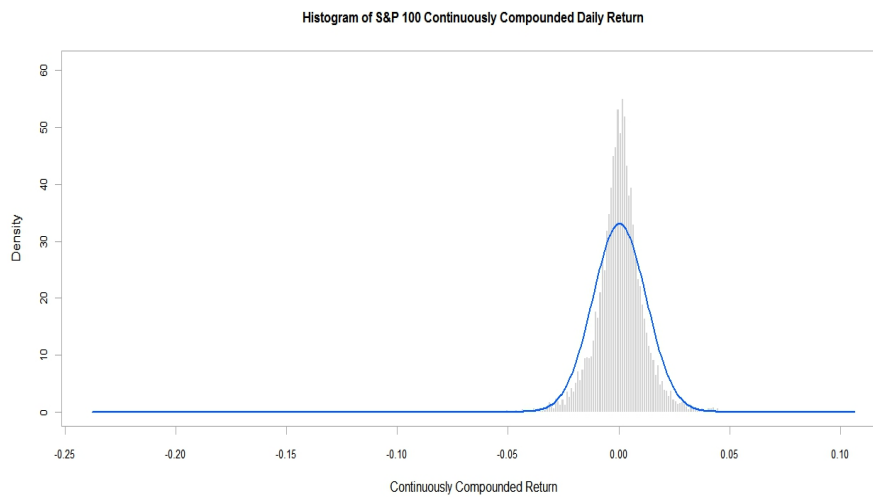
Figure 2.1: Histogram of CC S&P 100 Daily Return
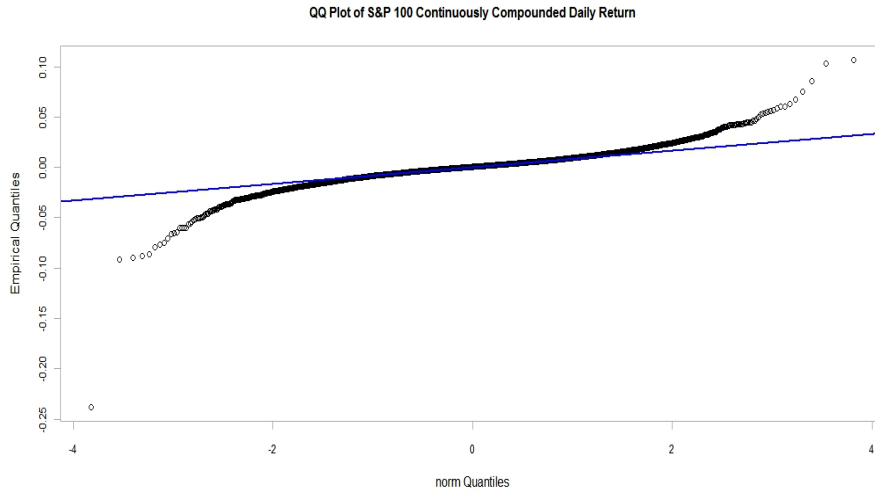
Figure 2.2: QQ plot of CC S&P 100 Daily Return

From the histogram, we can see that S&P 100 returns have higher and narrower peaks than those of the benchmark normal distribution. However, it is also not as symmetric as the normal lines. Also, the QQ-plot shows obvious deviation of the empirical quantile observations on both upper right side and lower left side of the drawn line, which implies that the empirical distribution has heavy tails. Furthermore, the sample skewness and kurtosis of S&P 100 are -1.1781 and 26.9880 receptively, while the skewness and kurtosis of a normal distribution are 0 and 3. Therefore, the empirical distribution of S&P 100 returns is not symmetric but negatively skewed, and heavy tailed. We conclude that the normal distribution is apparently not appropriate to characterize the empirical distribution of financial returns. Instead, we should look for some heavy tailed distributions.

2.8.2 Volatility Smile
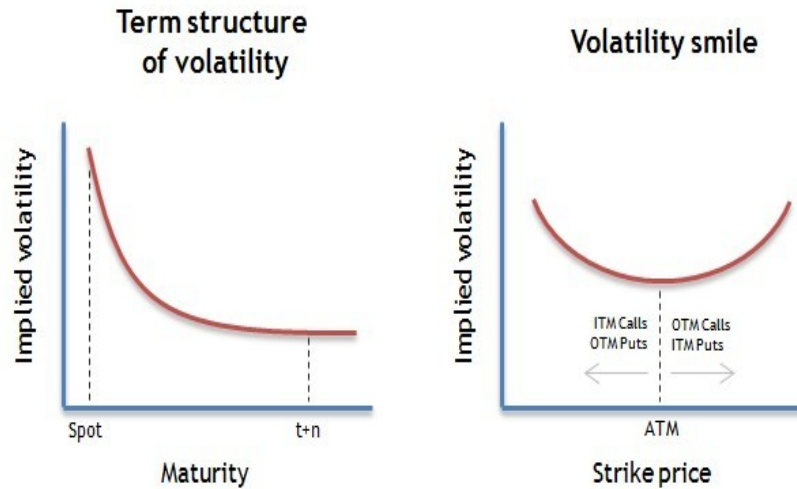
Figure 2.3: Volatility Smile

The Black-Scholes model assumes that volatility is constant over time, so the implied volatility should remain the same as both the strike price and the maturity change. However, volatility smile and volatility term [2.3] structure respectively demonstrate that implied volatility actually varies with strike price and maturity since 1987. We will further discuss the volatility smile phenomenon in the numerical result chapter.

2.8.3 Clustering and Leverage Effect
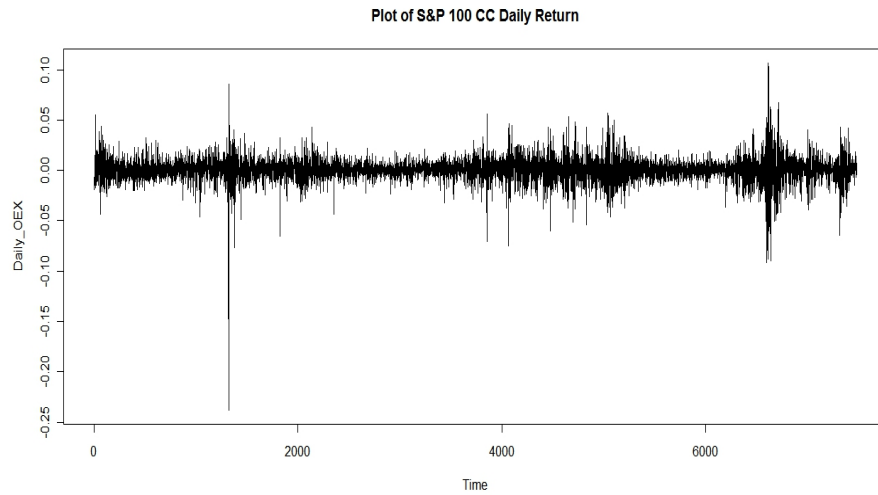
Figure 2.4: Continuously Compounded Daily Return of S&P 100
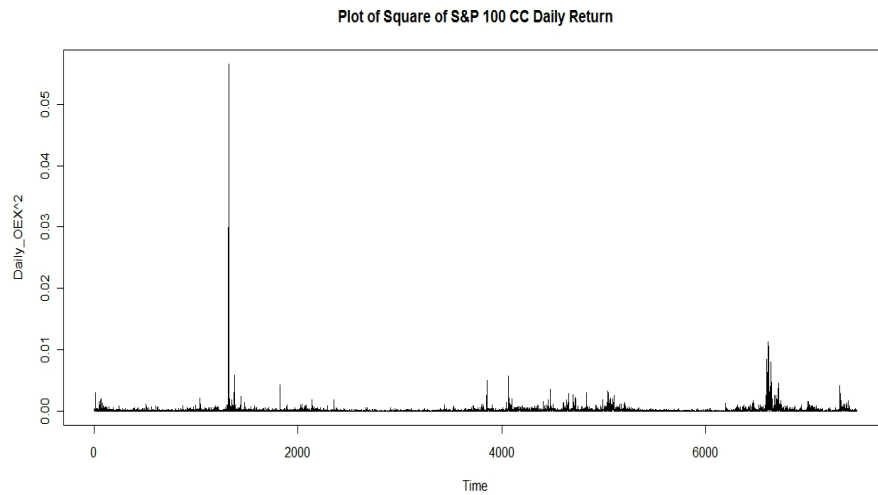
Figure 2.5: Square Value of Continuously Compounded Daily Return of S&P 100
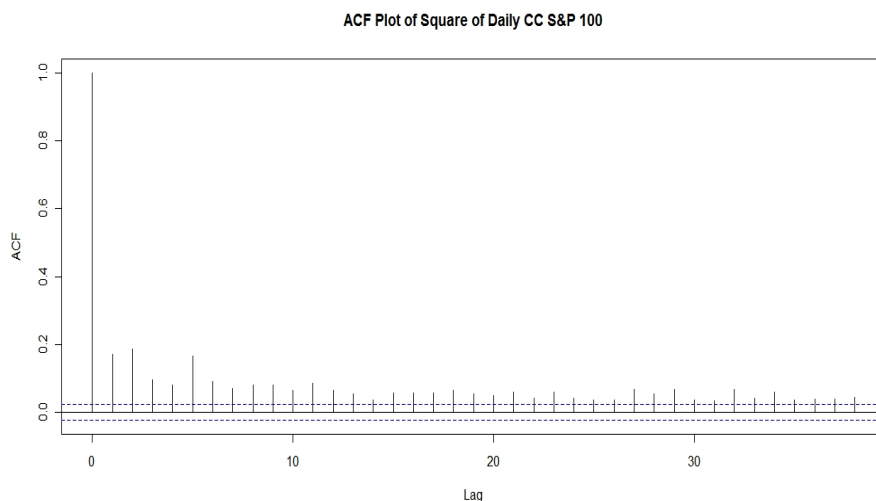
Figure 2.6: ACF Plot of Square of S&P100 Daily Return

In practice, it seems that the level of volatility of return (i.e. the fluctuations of the return) changes with time. Usually, periods of high (or low) volatility is immediately followed by subsequent periods of high (or low) volatility. Let us continue with the example of S&P100 Index. From the plot of the daily return, we can see that the periods of high volatility follow immediately after a large change in the level of the return. It is even more evident from the plot of the square of the daily returns. The sample autocorrelations coefficients of the squared returns are significantly different from 0 even at high lags, so that a shock to the volatility persists for many periods into the future. It provides strong evidence of the volatility clustering and correlation between volatility of daily return. Hence, we come to the conclusion that the assumption of constant volatility is counterfactual for financial asset returns.

Chapter 3

The Heston Model and Option Pricing

3.1 Heston's Stochastic Volatility Model

The Black-Scholes model approximately describes the behaviour of underlying asset prices and provides a convenient closed-form formula for option prices. It provides an important benchmark to evaluate the performance of other models. However, the assumptions of the Black-Scholes model are unrealistic due partly to its inability to generate the volatility smile and the skewness in the distribution of the return. Therefore, a variety of models are suggested to capture such properties of the return. In particular, Heston [16] has proposed a stochastic volatility model with a closed-form solution for the price of a European call option when the underlying assets are correlated with a latent volatility stochastic process. Below we review the Heston model.

Consider at time t the spot asset $S(t)$ which obeys a diffusion process:

$$dS(t) = \mu S dt + \sqrt{v(t)} S dW_1(t) \tag{3.1}$$

with volatility being treated as a latent stochastic process of Feller as proposed by Cox, Ingersoll and Ross [4]:

$$dv(t) = \kappa[\theta - v(t)]dt + \sigma \sqrt{v(t)} dW_2(t) \tag{3.2}$$

where $W_1(t)$ and $W_2(t)$ are both standard Wiener processes with a correlation coefficient given by $\rho > 0$:

$$dW_1(t)dW_2(t) = \rho dt$$

It is a mean reverting process related to the square-root process under the probability measure.[1] The variable μ is the instantaneous expected rate of return of the underlying asset, $\theta > 0$ is the long-term mean of the variance, $\kappa > 0$ is the speed of mean-reversion, i.e. the rate at which the variance converges to its long-run (or unconditional) mean level, $\sigma \geq 0$ represents the instantaneous volatility of the variance process $\{v(t)\} \geq 0$, ρ $(0 \leq \rho \leq 0)$ accounts for the correlation between the shocks driving the asset price and its instantaneous volatility, often interpreted as the *leverage effect*. There must exist a non-negative unique strong solution by the Yamada-Watanabe conditions [19]. For the square-root function which is not smooth at the origin, it is necessary to understand the behavior of the variance process at this point. The Feller classification of the boundaries for a one-dimensional diffusions process [20] implies the following:

- if $2\kappa\theta \geq \sigma^2$, then the origin is unattainable;

- if $2\kappa\theta < \sigma^2$, then the origin is a regular, attainable and reflecting boundary; this means that the variance process can touch 0 in finite times, but does not spend time there;

- infinity is a natural boundary, i.e. it can not be attained in finite times and the process can not be started there.

Under the probability measure, the derivatives is priced according to the risks since investors would require more profit for higher risks. Therefore, we need to add the price of risk to the expected return in order to price a derivative. However, the discounted rates differ among different investors based on their own attitudes to risk which are difficult to quantify. Fortunately, Cox and Ross (1976) [5] firstly introduce the risk-neutral valuation method. Later on, it was developed and formalized by Harrison and Kreps (1979) [12], Harrison and Pliska (1981, 1983) [13] [14] and Back and Pliska (1991)[1]. In a market free of arbitrage, we are able to price a derivative by taking the expected payoff under the risk-neutral probabilities instead of incorporating different investors' risk price. Now, we will explain how we transfer from the probability measure to the risk-neutral measure.

According to Fiorentini G., Leoń A. and Rubio G. [7], we need to incorporate the market price of volatility, λ, to switch from probability measure to the risk-neutral measure. The premium of volatility risk λ $(\lambda \in \mathbb{R})$ is defined as:

$$\lambda(S, V, t) = \lambda V_t$$

---

[1]As is pointed out by Nicolas Gisiger [10] "a probability measure is simply a mapping of outcomes to certain probabilities".

where V_t denotes the instantaneous variance. The Heston model under the risk-neutral measure is:

$$
\begin{aligned}
dS_t &= rS_t dt + \sqrt{V_t}S_t dW^*_{1t} \\
dV_t &= \kappa^*(\theta^* - V_t)dt + \sigma\sqrt{V_t}dW^*_{2t} \\
dW^*_{1t}dW^*_{2t} &= \rho dt
\end{aligned}
\tag{3.3}
$$

where $\kappa^* = \kappa + \lambda$, $\theta^* = \kappa\theta/(\kappa + \lambda)$.

3.2   European Option Pricing under the Heston Model

In a market free of arbitrage, it is demonstrated by Black and Scholes (1973), Merton (1973) that the value of any asset $U(S, v, t)$ must satisfy the PDE:

$$
\frac{1}{2}vS^2\frac{d^2U}{dS^2} + \rho\sigma vS\frac{d^2U}{dSdv} + \frac{1}{2}\sigma^2 v\frac{d^2U}{dv^2} + rs\frac{dU}{dS} + \{\kappa[\theta - v(t)] - \lambda v\}\frac{dU}{dv} - rU + \frac{dU}{dt} = 0 \tag{3.4}
$$

A European call option with a strike price K, maturing at time T is subject to the following conditions:

$$
\begin{aligned}
U(S, v, T) &= \max(0, S - K), \\
U(0, v, t) &= 0, \\
\frac{dU}{dS}(\infty, v, t) &= 1, \\
rS\frac{dU}{dS}(S, 0, t) + \kappa\theta\frac{dU}{dv}(S, 0, t) - rU(S, 0, t) + U_t(S, 0, t) &= 0, \\
U(S, \infty, t) &= S.
\end{aligned}
\tag{3.5}
$$

Due to the similar structure to the Black-Scholes model, Heston (1993) suggests that the solution should be of a similar form as:

$$
C(S, v, t) = SP_1 - KP(t, T)P_2 \tag{3.6}
$$

where the first term is the present value of the underlying asset, and the second term is the present value of the strike price. P_1 and P_2 should satisfy the PDE (3.16). For convenience, we write the PDE in terms of $X = \ln S$. Substituting the proposed solution (3.6) into the

original PDE (3.16), shows that P_1 and P_2 must satisfy the PDEs:

$$\frac{1}{2}v\frac{d^2P_j}{dx^2} + \rho\sigma v\frac{d^2P_j}{dxdv} + \frac{1}{2}\sigma^2 v\frac{d^2P_j}{dv^2} + (r+u_jv)\frac{dP_j}{dx} + (a_j - b_jv)\frac{dP_j}{dv} + \frac{dP_j}{dt} = 0, \qquad (3.7)$$

where
$u_1 = 1/2,\ \ u_2 = -1/2,\ \ a = \kappa\theta,\ \ b_1 = \kappa + \lambda - \rho\sigma,\ \ b_2 = \kappa + \lambda$ for j=1,2,. The European option price satisfies the boundary condition (3.5) and the PDEs (3.7) are constrained to the terminal condition:

$$P_j(S, v, T; \ln[K]) = 1_{\{S \geq \ln[K]\}} \tag{3.8}$$

The characteristic function solution is:

$$f_j(S, v, t; \Phi) = e^{C(T-t;\Phi) + D(T-t;\Phi)v + i\Phi S}, \tag{3.9}$$

where

$$
\begin{aligned}
C(\tau; \Phi) &= r\Phi i\tau + \frac{a}{\sigma^2}(b_j - \rho\sigma\Phi i + d)\tau - 2\ln\left[\frac{1 - ge^{d\tau}}{1 - g}\right], \\
D(\tau; \Phi) &= \frac{b_j - \rho\sigma\Phi i + d}{\sigma^2}\left[\frac{1 - e^{d\tau}}{1 - ge^{d\tau}}\right], \\
g &= \frac{b_j - \rho\sigma\Phi i + d}{b_j - \rho\sigma\Phi i - d} \\
d &= \sqrt{(\rho\sigma\Phi i - b_j)^2 - \sigma^2(2u_j\Phi i - \Phi^2)}.
\end{aligned}
\tag{3.10}
$$

After some conversion of the characteristic function (3.9), we obtain the conditional probability that the option expires in-the-money:

$$P_j(S, v, T; \ln[K]) = \frac{1}{2} + \frac{1}{\pi}\int_0^\infty Re\left[\frac{e^{-i\phi\ln[K]}f_j(S, v, T; \Phi)}{i\phi}\right]d\phi \tag{3.11}$$

The final solution consists of [3.6], [3.9] and [3.11]. [3.11] may be interpreted as "adjusted" or "risk-neutralized" probability. The integrand in equation [3.11] is a "smooth function that decays rapidly" and it is integrable as shown by Kendall and Stuart(1977) [21]. Its integrand can not be evaluated analytically, but it can be approximated numerically.

3.3   American Option Pricing under Heston Model

First, let us define t a time to expiration. In the Heston model, the stock price and volatility follows the following stochastic differential equations:

$$
\begin{aligned}
dS(t) &= \mu S dt + \sqrt{v(t)} S dW_1(t) \\
dv(t) &= \kappa[\theta - v(t)]dt + \sigma\sqrt{v(t)}dW_2(t)
\end{aligned}
\tag{3.12}
$$

with

$$
dW_1(t)dW_2(t) = \rho dt
\tag{3.13}
$$

For the American Put Option, the payoff is:

$$
u(S, v, T) = \max(K - S, 0)
\tag{3.14}
$$

where K is the exercise price. An American put option with a strike price K and maturing at time T satisfies the PDE (3.16) subject to the boundary conditions:

$$
\kappa\theta\frac{\partial U(0,0,t)}{\partial v} - rU(0,0,t) + \frac{\partial U(0,0,t)}{\partial t} = 0
$$

$$
\frac{1}{2}vS^2\frac{\partial^2 U(0,v,t)}{\partial S^2} + [\kappa(\theta - v(t) - \lambda(S,v,t)]\frac{\partial U(0,v,t)}{\partial v} - rU(0,v,t) + \frac{\partial U(0,v,t)}{\partial t} = 0
$$

$$
\frac{\partial U(S, +\infty, t)}{\partial S} = 0
$$

$$
\frac{\partial U(+\infty, v, t)}{\partial S} = 0
$$

$$
u(S, v, t) \geq \max(K - x, 0) := g(S)
\tag{3.15}
$$

3.3.1   Alternating Direction Implicit Method

In section 2.6.7 we utilized the PSOR method in solving the Black-Scholes differential equation which is a two-dimensional problem. However, when it comes to a three dimensional problem, PSOR tends to converge very slowly. Hence, here we consider the Alternating Direction Implicit Method (ADI) in solving the Heston's Differential Equation. ADI, which is an example of an Operator Splitting Method, was firstly introduced by Peaceman and Rachford [24] in 1955. From then on, it has been successfully applied in many areas to solve PDE without a mixed spatial derivative term. Hout and Foulon [17] adapted several

ADI schemes to solve the Heston PDE with a mixed derivative term for European option prices. Fjelland [8] further updated the ADI scheme for European option pricing. Recall that any price of any contingent claim on a underlying stock S satisfies the following PDE:

$$\frac{1}{2}vS^2\frac{d^2U}{dS^2} + \rho\sigma vS\frac{d^2U}{dSdv} + \frac{1}{2}\sigma^2 v\frac{d^2U}{dv^2} + rs\frac{dU}{dS} + \{\kappa[\theta - v(t)] - \lambda v\}\frac{dU}{dv} - rU + \frac{dU}{dt} = 0 \quad (3.16)$$

In order to solve for the price of the American Put option, we have to solve the PDE (3.16) together with the above boundary conditions.

Let us rewrite the PDE (3.16) as follows:

$$0 = \frac{\partial U}{\partial t} + A_{vS}U + A_S U + A_v U \quad (3.17)$$

where

$$A_{vS} = \rho v\sigma S\frac{\partial}{\partial S\partial v} \quad (3.18)$$

$$A_S = \frac{1}{2}vS^2\frac{\partial^2}{\partial S^2} + rS\frac{\partial}{\partial S} \quad (3.19)$$

$$A_v = \frac{1}{2}\sigma^2 v\frac{\partial^2}{\partial v^2} + \kappa(\eta - v)\frac{\partial}{\partial v} - r \quad (3.20)$$

Here we use the ADI scheme proposed by Fjelland [8].

$$
\begin{aligned}
0 &= \frac{U^{t+\Delta t} + U^{t+\frac{1}{2}\Delta t} - U^{t+\frac{1}{2}\Delta t} - U^t}{\Delta t} \\
&+ \frac{1}{2}\left(A_S U^{t+\frac{1}{2}\Delta t} + A_v U^{t+\Delta t} + A_S U^{t+\frac{1}{2}\Delta t} + A_v U^t + 2A_{vS}U^{t+\Delta t}\right) \quad (3.21)
\end{aligned}
$$

Next we rearrange the terms in the above equation to end up with:

$$0 = \frac{U^{t+\Delta t} - U^{t+\frac{1}{2}\Delta t}}{\Delta t} + \frac{1}{2}\left(A_v U^{t+\Delta t} + A_S U^{t+\frac{1}{2}\Delta t} + 2A_{vS}U^{t+\Delta t}\right) \quad (3.22)$$

$$\frac{U^{t+\frac{1}{2}\Delta t} - U^t}{\Delta t} + \frac{1}{2}\left(A_S U^{t+\frac{1}{2}\Delta t} + A_v U^t\right) \quad (3.23)$$

28

Setting (3.24) and (3.23) to be zero respectively, we get:

$$0 \;=\; \frac{U^{t+\Delta t} - U^{t+\frac{1}{2}\Delta t}}{\Delta t} + \frac{1}{2}\left(A_v U^{t+\Delta t} + A_S U^{t+\frac{1}{2}\Delta t} + 2A_{vS}U^{t+\Delta t} \right) \tag{3.24}$$

$$0 \;=\; \frac{U^{t+\frac{1}{2}\Delta t} - U^{t}}{\Delta t} + \frac{1}{2}\left(A_S U^{t+\frac{1}{2}\Delta t} + A_v U^{t} \right) \tag{3.25}$$

By inserting (3.18), (3.19) and (3.20) into (3.24) and (3.25), we obtain

$$h_{ij}(U^{n+1}_{i+1,j+1} - U^{n+1}_{i+1,j-1} - U^{n+1}_{i-1,j+1} + U^{n+1}_{i-1,j-1})$$
$$+a_j U^{n+1}_{i+1,j} + b_j U^{n+1}_{i,j} + c_j U^{n+1}_{i-1,j} \;=\; \alpha_{ij} U^{n+\frac{1}{2}}_{i,j+1} + \beta_{ij} U^{n+\frac{1}{2}}_{i,j} + \gamma_{ij} U^{n+\frac{1}{2}}_{i,j-1} \tag{3.26}$$
$$d_{ij} U^{n+\frac{1}{2}}_{i,j+1} + e_{ij} U^{n+\frac{1}{2}}_{i,j-1} + f_{ij} U^{n+\frac{1}{2}}_{i,j-1} \;=\; \kappa_j U^{n}_{i+1,j} + \lambda_j U^{n}_{i,j} + \mu_j U^{n}_{i-1,j} \tag{3.27}$$

where

$$
\begin{aligned}
h_{ij} &= \frac{\rho v_j \sigma S_i}{4\Delta S \Delta v} \\[4pt]
a_j &= \frac{\sigma^2 v_j}{2\Delta v_j^2} + \frac{\kappa(\eta - v_j)}{2\Delta v} & \alpha_{ij} &= -d_{ij} \\[4pt]
b_j &= \frac{2}{\Delta t} - \frac{\sigma^2 v_j}{\Delta v^2 - r} & \beta_{ij} &= -e_{ij} + \frac{4}{\Delta t} \\[4pt]
c_j &= \frac{\sigma^2 v_j}{2\Delta v_j^2} - \frac{\kappa(\eta - v)}{2\Delta v} & \gamma_{ij} &= -f_{ij} \\[4pt]
d_{ij} &= \frac{v_j S_i^2}{2\Delta S^2} + \frac{r S_i}{2\Delta S} & \kappa_j &= -a_i \\[4pt]
e_{ij} &= \frac{2}{\Delta t} - \frac{v_j S_i^2}{\Delta S^2} & \lambda_j &= -b_j + \frac{4}{\Delta} \\[4pt]
f_{ij} &= \frac{v_j S_i^2}{2\Delta S^2} - \frac{r S_i}{2\Delta S} & \mu_j &= -c_i
\end{aligned}
\tag{3.28}
$$

It is found that h_{ij}, d_{ij}, e_{ij} and f_{ij} depends on both the level of S and the level of v, which makes it impossible to construct a tridiagonal matrix as is done for the derivative terms with regards to S. To sovle this problem, Fjelland (2012) [8] suggested splitting the columns in v so that every new array contains only v's at one level of S. Every new array has one tridiagonal matrix assosiated with it, then we can use Tridiagonal Matrix Algorithm to implicitly compute all arrays in a fast way. In the next section, we are going

to discuss about Tridiagonal Matrix Algorithm in details.

Tridiagonal Matrix Algorithm - TDMA (Thomas algorithm)

The Tridiagonal matrix algorithm (TDMA) [26] is used to solve the tridiagonal system of equations.

$$
\begin{pmatrix}
b_1 & c_1 & \ldots & \ldots & 0 & 0 \\
a_2 & b_2 & c_2 & 0 & \ldots & 0 \\
\vdots & \vdots & \vdots & \vdots & \vdots & \vdots \\
0 & \ddots & a_i & b_i & c_i & \ddots \\
0 & 0 & \ldots & \ldots & a_m & b_m
\end{pmatrix}
\times
\begin{pmatrix}
U_1^{n+1} \\
U_2^{n+1} \\
\vdots \\
U_i^{n+1} \\
U_m^{n+1}
\end{pmatrix}
=
\begin{pmatrix}
U_1^n \\
U_2^n \\
\vdots \\
U_i^n \\
U_m^n
\end{pmatrix}
$$

Basically, we are solving a system of equations of the following form:

$$
\begin{align}
a_1 x_0 + b_1 x_1 + c_1 x_2 &= y_1 \tag{3.29} \\
a_2 x_1 + b_2 x_2 + c_2 x_3 &= y_2 \tag{3.30} \\
a_3 x_2 + b_3 x_3 + c_3 x_4 &= y_3 \tag{3.31} \\
&\ldots\ldots\ldots \notag \\
a_n x_{n-1} + b_n x_n + c_n x_{n+1} &= y_n \tag{3.32} \\
&\tag{3.33}
\end{align}
$$

where $x_0 = 0$ and $x_{n+1} = 0$. The TDMA mainly involves two steps: the first steps is to do some row operations to eliminate the lower triangular of the tridiagonal matrix; and the second step is to do a backward substitution to solve for each x_i. More specifically, for the elimination step, we multiply the i_{th} row by b_{i-1} and then subtract the i_{th} row multiplied by a_i. For example, we apply this to the first two rows and end up with

$$
(b_2 b_1 - a_2 c_1) x_2 + c_2 b_1 x_3 = y_2 b_1 - y_1 a_2
$$

Therefore, we eliminate the x_1 term in the second row. We repeatedly apply the same algorithm to all the rows and it results in a matrix of the following format.

$$\begin{pmatrix} \hat{b}_1 & \hat{c}_1 & \dots & \dots & 0 & 0 \\ 0 & \hat{b}_2 & \hat{c}_2 & 0 & \dots & 0 \\ \vdots & \vdots & \vdots & \vdots & \vdots & \vdots \\ 0 & \ddots & 0 & \hat{b}_i & \hat{c}_i & \ddots \\ 0 & 0 & \dots & \dots & 0 & \hat{b}_m \end{pmatrix} \times \begin{pmatrix} U_1^{n+1} \\ U_2^{n+1} \\ \vdots \\ U_i^{n+1} \\ U_m^{n+1} \end{pmatrix} = \begin{pmatrix} U_1^n \\ U_2^n \\ \vdots \\ U_i^n \\ U_m^n \end{pmatrix}$$

where $\hat{b}_1 = 1; \hat{c}_1 = c_1$ For the n_{th} row, the unknown variable is only x_n. We can then substitute the value back into the $n-1_{th}$ row and solve for x_{n-1}. Hence, we can recursively solve for all the $x_i's$. If we set the recursive formula to be:

$$x_i = \gamma_i x_{i+1} + \beta_i \tag{3.34}$$

Multiply (3.34) by a_i and subtract it from the i_{th} row:

$$x_i = \frac{-c_i}{b_i + \gamma_i a_i} x_{i+1} + \frac{y_i - a_i \beta_i}{b_i + \gamma_i a_i}$$

Therefore,

$$\gamma_{i+1} = \frac{-c_i}{b_i + \gamma_i a_i}, \quad \beta_{i+1} = \frac{y_i - a_i \beta_i}{b_i + \gamma_i a_i}$$

We state as before that $x_{n+1} = 0$. Substitute this into (3.34), we get

$$x_n = \beta_n = \frac{y_{n-1} - a_{n-1}\beta_{n-1}}{b_{n-1} + \gamma_{n-1}a_{n-1}} \tag{3.35}$$

We can get γ_0 and β_0 from

$$a_1 x_0 + b_1 x_1 + c_1 x_2 = y_1 \tag{3.36}$$

Since $x_0 = 0$, we arrange the terms in the above equation to get

$$\gamma_1 = -\frac{c_1}{b_1}, \quad \beta_1 = \frac{y_1}{b_1}$$

31

3.4 Calibration of the Heston Model

In section 3.1, we has introduced the Heston model under the probability measure and also discussed about transferring from the probability measure to the risk-neutral measure by incorporating the the premium of volatility risk λ. Now we are going to discuss about how we calibrate the Heston's option pricing model.

Basically, we employ a two-step procedure suggested by Fiorentin, Leoń and Rubio [7] in calibrating the option pricing model. The first step is to calibrate the diffusion parameters $\Omega = (\mu, \kappa, \theta, \sigma, \rho)$ by the indirect inference method using the historical stock prices. Then, in the second step, we estimate the premium of volatility risk λ and the instantaneous variance V_t by the least squares method with the market option prices. Then, we can incorporate λ into the Heston model according to (3.3) in order to transfer from the probability measure to the risk-neutral measure.

3.4.1 Estimation of the Diffusion Parameters

We are going to focus on the indirect inference method being used to estimate Ω in the first step. The indirect inference method is first proposed by Gouriéroux [11]. As we know that after we apply a discrete-time approximation to the continuous process, an estimator of Ω obtained from a pseudo maximum likelihood, or generalized method of moments would produce bias. Hence, Fiorentin, Leoń and Rubio (2002) propose an indirect inference method for estimating the parameters in the Ω vector which corrects for the bias in the resulting parameter estimates of the discrete-time approximation models. The core idea is to match moments of the auxiliary model from simulated data to the observed data. The second step is to estimate the volatility risk premium λ and the instantaneous volatility V_t from the option prices. However, there is a legitimate question as to whether the implied parameters we obtain from market option prices are consistent with the diffusion process fitted with the observed stock returns.

Indirect Inference Procedure

Note that Fiorentin, Leoń and Rubio (2002) [7] did not directly use the Heston model introduced in section 3.1. Instead, they take a logarithm of the original stock price S. Below we are going to show the indirect inference procedure in details.

Consider at time t the spot asset returns $x_t \equiv \ln S_t$ obey a diffusion process which is similar to the stochastic differential equation used in Black-Scholes model:

$$dx_t = \sqrt{V_t}dW_{1t} \tag{3.37}$$

Suppose that its variance follows the Feller diffusion process (or a CIR process) proposed by Cox, Ingersoll and Ross [4]:

$$dV_t = \kappa(\theta - V_t)dt + \sigma\sqrt{V_t}dW_{2t} \tag{3.38}$$

where W_{1t} and W_{2t} are both Wiener processes with a correlation coefficient of $\rho > 0$:

$$dW_{1t}dW_{2t} = \rho dt$$

where $\Omega = (\mu, \kappa, \theta, \sigma, \rho)$.

All of the data we observe from the financial market are discrete, however, the models are built in the continuous time framework. Therefore, we need to apply a discretization scheme.
The following is Euler discretization scheme:

$$x_t = x_{t-\tau} - \frac{V_{t-\tau}}{2}\tau + \sqrt{V_{t-\tau}\tau}\eta_{1t} \tag{3.39}$$

$$V_t = \kappa\theta\tau + (1 - \kappa\tau)V_{t-\tau} + \sigma\sqrt{V_{t-\tau}\tau}\zeta_t \tag{3.40}$$

$$\zeta_t = \rho\eta_{1t} + \sqrt{1 - \rho^2}\eta_{2t} \tag{3.41}$$

where $(\eta_{1t}, \eta_{2t})' \sim i.i.d\ N(0, I)$.
An immediate problem with the scheme above is that the discrete process for V_t can become negative with non-zero probability, which in turn would make the computation of $\sqrt{V_t}$ impossible and cause the time-stepping scheme to fail. To get around this problem, we apply full truncation in out code, which is $V_t^+ = \max(V_t, 0)$.

Below we discuss how to implement the indirect inference method. First, we estimate the parameter vector ψ of the auxiliary model by the method of pseudo maximum likelihood. Let us denote the estimates computed from the original observed stock returns as $\hat{\psi}_T$. Second, for a given Ω, we can simulate a series of returns from the stochastic process, and then we fit an auxiliary model with the simulated data. Here, we denote the new estimates obtained from the simulated data as $\tilde{\psi}(\Omega)$. The estimate of $\hat{\Omega}$ should be the one that makes the distance between the two estimated ψ as small as possible. In this way, the simulated stock returns from the Heston model with an estimated parameter vector $\hat{\Omega}$

would be mostly similar to the observed stock returns. So the indirect inference estimate of Ω is obtained as:

$$\hat{\Omega} = \underset{\Omega}{\operatorname{argmin}}(\hat{\psi}_T - \frac{1}{N}\sum_{i=1}^{N}\tilde{\psi}(\Omega))'W(\hat{\psi}_T - \frac{1}{N}\sum_{i=1}^{N}\tilde{\psi}(\Omega)) \tag{3.42}$$

where W is an optimal weighting matrix:

$$W = \frac{1}{N}\sum_{t=1}^{N}\frac{dl_t(r_t,\Omega)dl_t(r_t,\Omega)}{d\Omega d\Omega'} \tag{3.43}$$

Note that if dimΩ=dimψ, the weighting matrix reduces to $W = I$ where I is the identity matrix.

Auxiliary Model

For different American put options, we might need different auxiliary model to best fit the stock returns since different models have different specialties. Basically, we are considering the models in the Generalized Autoregressive Conditional Heteroskedasticity (GARCH) family. Here are several choices for an auxiliary model.

Conditional Mean Equation

$$r_t = \mathbb{E}_{t-1}[r_t] + \varepsilon_t, \varepsilon_t = \sigma_t z_t; z_t|I_t \sim i.i.d \ N(0,1) \tag{3.44}$$

Conditional Variance Equation

The standard Generalized Autoregressive Conditional Heteroskedasticity of order q and p (GARCH(q,p)) model (Bollerslev (1986)) is given by:

$$\sigma_t^2 = \left(\omega + \sum_{j=1}^{m}\zeta_j v_{jt}\right) + \sum_{j=1}^{q}\alpha_j\varepsilon_{t-j}^2 + \sum_{j=1}^{p}\beta_j\sigma_{t-j}^2 \tag{3.45}$$

where σ_t^2 denotes the conditional variance, ω represents the intercept term and q captures the lag dependence of previous squared innovations and p captures the lag dependence of previous squared volatilities, v_j is a $m \times 1$ vector of exogenous explanatory variables that can include binary variables and other relevant explanatory variables and δ is a $m \times 1$ vector of positive coefficients. We assume that $\omega > 0$, $\alpha_j \geq 0$ and $\beta_j \geq 0$ to ensure nonnegativity of conditional variance. Besides, we also assume that $\sum_{j=1}^{q}\alpha_j + \sum_{j=1}^{p}\beta_j < 1$ so that the

34

ε_t is a stationary and ergodic martingale difference series with finite variance. $\varepsilon_t = \sigma_t z_t$ is a multiplicative error. Generally, the random variance z_t does not have to be normally distributed. It can have a fat-tailed distribution such as Student t distribution. However, in this thesis, we assume it follows standard normal distribution for simplicity.

The conditional mean $\mathbb{E}_{t-1}[r_t] = c$ or $\mathbb{E}_{t-1}[r_t] = \text{ARMA(r,s)}$ for low order of r autoregressive lags and s moving average lags to capture potential autocorrelation caused by market microstructure effects (e.g., bid-ask bounce) or non-trading effects. If extreme or unusual market events have happened during sample period, then dummy variables associated with these events can be added to the conditional mean specification to remove these effects.

The Nelson's exponential GARCH (EGARCH) Model is given by:

$$ln(\sigma_t^2) = \left(\omega + \sum_{j=1}^{m} \zeta_j v_{jt}\right) + \sum_{j=1}^{q}(\alpha_j z_{t-j} + \gamma_j(|z_{t-j}| - E|z_{t-j}|)) + \sum_{j=1}^{p} \beta_j ln(\sigma_{t-j}^2) \quad (3.46)$$

where the coefficient α_j captures the sign effect with $\alpha_j < 0$ being taken as evidence for the presence of the leverage effect in the data and γ_j captures the size effect with $\gamma_j > 0$ implying a larger leverage effect. EGARCH model is covariance stationary provided $\sum_{j=1}^{q} b_j < 1$

The Nonlinear Asymmetric GARCH(NAGARCH) is defined as:

$$\sigma_t^2 = \left(\omega + \sum_{j=1}^{m} \zeta_j v_{jt}\right) + \sum_{j=1}^{q} \alpha_j \sigma_{t-1}^2(|z_{t-j} - \eta_{2j}|)^2 + \sum_{j=1}^{p} \beta_j \sigma_{t-j}^2 \quad (3.47)$$

The Threshold GARCH (TGARCH) model is:

$$\sigma_t = \left(\omega + \sum_{j=1}^{m} \zeta_j v_{jt}\right) + \sum_{j=1}^{q} \alpha_j \sigma_{t-1}(|z_{t-j}| - \eta_{1j} z_{t-j}) + \sum_{j=1}^{p} \beta_j \sigma_{t-j} \quad (3.48)$$

where $|\eta_{1j}| \leq 1$.

3.4.2 Estimation of Volatility Premium and Instantaneous Volatility

The next step is to estimate volatility premium λ and the implied volatility with the corresponding option data. Define the price error between the estimated price and true

observed option price as:

$$e_{it}(V_t, \lambda; \hat{\Omega}_t) = \hat{c}_{it}(K_i) - c_{it}(K_i) \tag{3.49}$$

where $\hat{c}_{it}(K_i)$ is the theoretical price of the call i in day t, and $c_{it}(K_i)$ is the corresponding observed market price. Then we want to minimize the pricing error to solve for λ and V_t. We apply a least squares method here, that is we minimize $\sum_{i=1}^{N} e_{it}^2(V_t, \lambda; \hat{\Omega}_t)$ with respect to V_t and λ at time t.

Chapter 4

Numerical Result

4.1 The Application of the Heston Model to the American Options

Let us fix $T = 0.25$; $\sigma = 0.9$; $\kappa = 5$; $\theta = 0.16$; $\rho = 0.1$; $r = 0.1$; $K = 10$; $S_0 = 10$; $V_t = 0.0625$. Next we change one of the variables at a time and see how the American put option changes as this particular variable changes under the Heston model.

1. Change the spot stock price from 8 to 12. Figure 4.1 shows that for a put option, the price decreases when the underlying price, S, increases as expected.
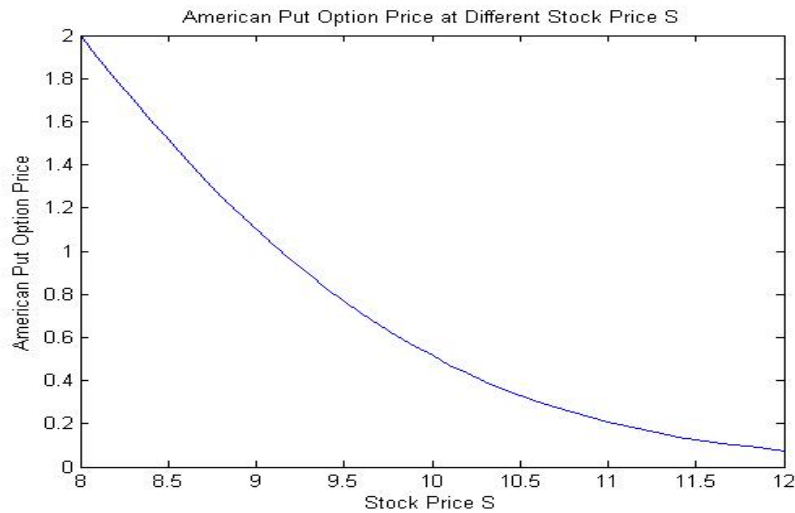
Figure 4.1: American Put Price under different Stock Prices

2. Change the instantaneous variance V_t from 0 to 0.5. Figure 4.2, Figure 4.3, Figure 4.4 respectively show the volatility square, V_t, has a positive effect on the American-style option price, the larger the volatility, the higher the price. All three figures have the same increasing trend indicating that the option prices increases as V_t increases. However a closer look at Figures 4.2, Figure 4.3 and Figure 4.4 reveals that across all the moneyness, the at-the-money options are most affected by V_t. In addition, the change of V_t form 0 to 0.5 seems to induce the largest price difference for at-the-money options. This is likely due to the fact that the at-the-money options are most sensitive to the market, not only affected by the underlying price, but also by a variety of market indices.
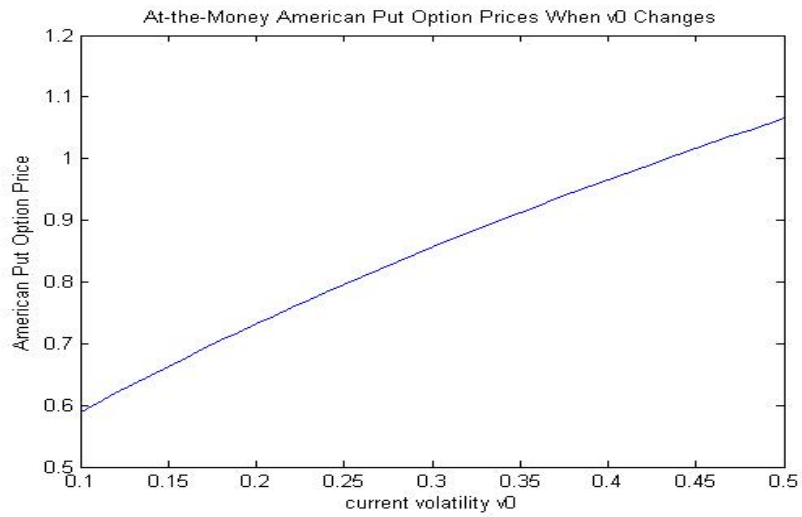
Figure 4.2: At-the-Money Put Price under Different Instantaneous Volatility V_t
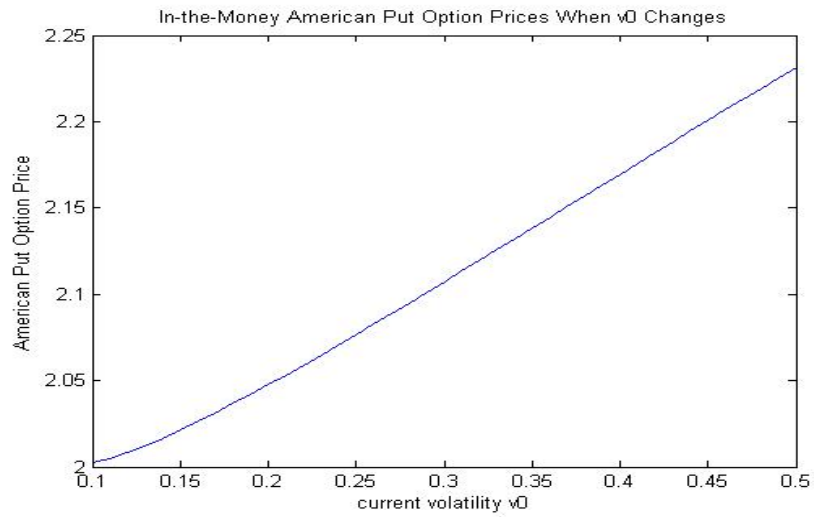
Figure 4.3: In-the-Money Put Option at Different Instantaneous Volatility V_t
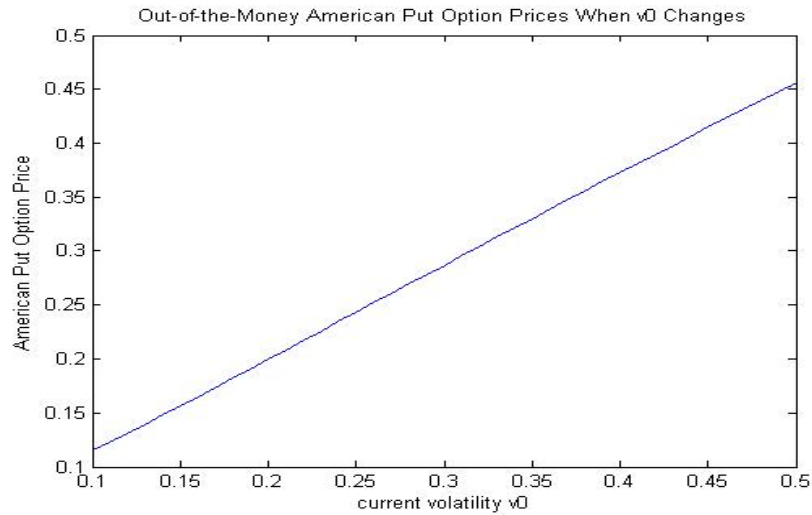
Figure 4.4: Out-of-the-Money American Put Price at different Instantaneous Volatility V_t

Figure 4.5 shows the prices of a European and an American put option generated by Heston model for parameter values $T = 1$; $K = 1$; $\kappa = 0.75$; $\theta = 0.46$; $\sigma = 2.78$; $\rho = -0.64$; $\lambda = -0.02$; and $r = 0.02$. The result is consistent with that of the Black-Scholes model. It shows that both the European put option price and the American option price decline as in addition the stock price S grows and they are approaching zero when S is large enough. Also the American option has higher price than the European option does and we also observe that the price differences between the American put option and the European put option is decreasing as S increases.
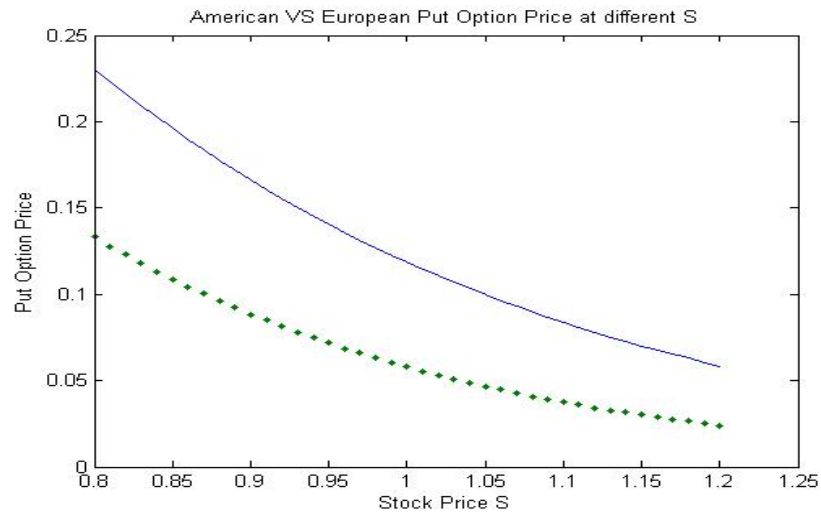
Figure 4.5: American Put Price

Now let $T = 1$; $K = 1$; $\kappa = 0.75$; $\theta = 0.46$; $\sigma = 2.78$; $\rho = -0.64$; $\lambda = -0.02$; and $r = 0.02$. Change one parameter at a time and hold others constant to assess the effect of the six structure parameters on option pricing:

Parameters	values	$V_t = 0.05$	$V_t = 0.2$
	0.02	0.0747	0.1383
κ	0.75	0.1079	0.1791
	2	0.1148	0.2106
	0.04	0.0627	0.1153
θ	0.46	0.1079	0.1791
	0.92	0.1136	0.2034
	-0.02	0.1079	0.1791
λ	0	0.1079	0.1790
	0.02	0.1079	0.1790
	0	0.1156	0.1857
r	0.02	0.1079	0.1791
	0.2	0.0610	0.1339
	0.5	0.1130	6.1032
σ	2.78	0.1079	0.1791
	5	0.1072	0.1736

Table 4.1: American Put Option Price Under Heston Model

Each time, we change one parameter while holding other parameters constant. The first columns contains the parameters to be changed. The second column is the value of the changing parameter. The third and forth columns are the American Put option prices under each changed parameters with instantaneous volatility $V_t = 0.05$ and $V_t = 0.2$ respectively.

Table 4.1 demonstrates that a large value of κ and θ leads to a higher option price under different V_t. The option price is not sensitive to λ since all option prices are of the same under different values of λ. As we increase r and σ, the option decreases. Also, a larger V_t always results in a larger option price.

4.2 Volatility Smiles

4.2.1 American Option

Consider an American put option on an underlying $S = 1$ with one year to maturity; in order to study the volatility smile, different strike prices are required. The strike prices have to be chosen carefully to avoid too large or too small values. If the strike price is too high compared with the underlying price, the option would be deep in-the-money and fall

into the early exercise region. On the other hand, if the strike is too low, the option would be deep out-of-the-money, which has little value. Either case could cause the failure of the option pricing model.

After deciding for the range of values of the strike prices, the Heston model is used to calculate the option prices with respect to each strike price. Once an option price is calculated, this together with the current strike price, interest rate and underlying price are fitted to the Black-Scholes model to calculate the implied volatility. This implied volatility is then the value for the corresponding strike price. This procedure is repeated in calculating the implied volatility for a number of different strike prices. A curve of volatility smile is then completed by plotting the data pairs, (strike, implied volatility), onto the coordinates.

Figure 4.6 is the implied volatility of an American put options for $T = 1$; $S = 1$; $\theta = 0.46$; $\sigma = 2.78$; $\rho = -0.64$; $\lambda = -0.02$; $r = 0.02$; $\kappa = 0.05$; 0.75 and 2. It shows that a higher κ results in a higher implied volatility. The effect is more obvious for the in-the-money options than the extreme wings of the curves. The pattern that implied volatility changes faster as the option goes from out-of-the-money to in-the-money is known in the literature as a "volatility sneer". Also, the skewness pattern in Figure 4.6 is persistent across all moneyness.

Figure 4.6: Implied Volatility of American Put Option Under Heston Model

Figure 4.7 is the implied volatility of an American put options for $T = 1$; $S = 1$; $\theta = 0.46$ and 0.72; $\sigma = 2.78$; $\rho = -0.64$; $\lambda = -0.02$; $r = 0.02$; $\kappa = 0.75$. As θ is the average

of long term mean, the higher the variance, the higher the volatility. Furthermore, this pattern is more noticeable for in-the-money options than options of other moneyness.

Figure 4.7: Implied Volatility of American Put Option Under Heston Model

Figure 4.8 is the implied volatility of an American put options for $T = 1$; $S = 1$; $\theta = 0.46$; $\sigma = 2.78$; $\rho = -0.64$; 0 and 0.64; $\lambda = -0.02$; $r = 0.02$; $\kappa = 0.75$. It depicts the not-so-symmetric volatility smiles known as: a volatility sneer. The non-smooth curves are caused by the same effect describes before. The uncorrelated case, $\rho = 0$, produces a curve that looks like a relatively symmetric smile centered at-the-money. However, it would not be exactly symmetric, as changing ρ would change the degree of symmetry. In particular, negative correlation results in a higher implied volatility for the out-of-the-money put options while positive correlation leads to a higher implied volatility for the in-the-money put options.

Consider an American put option, when it moves from out-of-the-money to at-the-money, here the underlying price gradually decreases. If the correlation is negative, then the variance will increase, which results in higher implied volatility. On the other hand, if the correlation is positive, the variance will decrease with the increase of S, and this would reduce the implied volatility. This explains the first segment of the figure. For the second segment of the figure when the option is in the money, if it moves from in-the-money to at-the-money, the underlying price would increase. In this case, if the correlation is positive, the variance would increase with S, and thus results in a higher implied volatility.

However, if the correlation is negative, the variance decreases and results in a lower implied volatility.
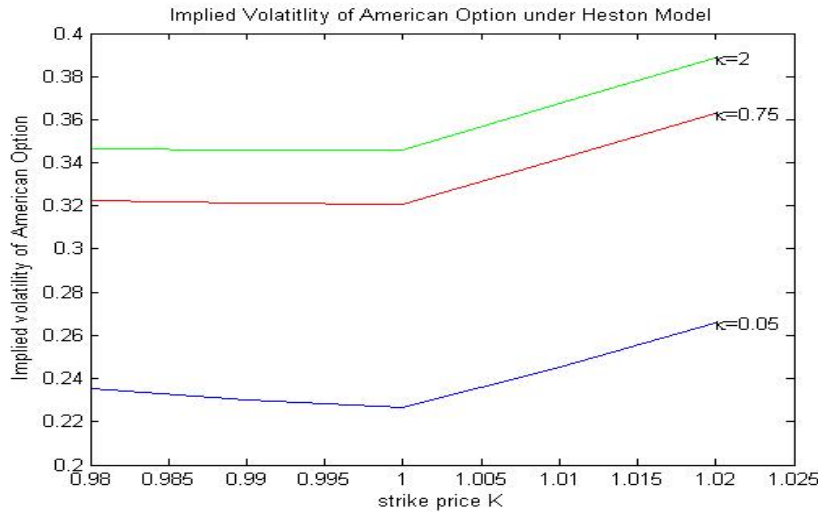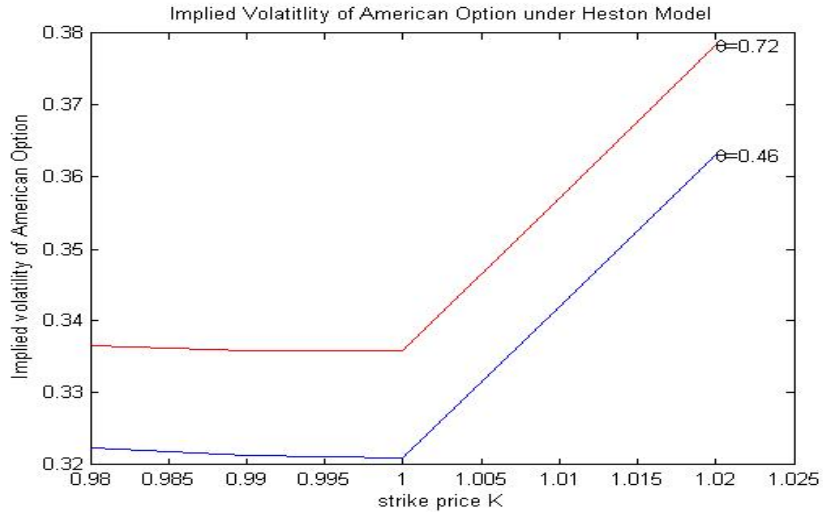

Figure 4.8: Implied Volatility of American Put Option Under Heston Model

Figure 4.9 is the implied volatility of an American put options for $T = 1$; $S = 1$; $\theta = 0.46$; $\sigma = 2.78$; $\rho = -0.64$; $\lambda = -0.02$; $r = 0$; 0.02; and 0.04; $\kappa = 0.75$ and $\kappa = 2$. Three different values of λ, market price of risk, are tested with other parameters held constant. The three curves are approximately parallel to each other, which indicates that the change of λ has an equal effect on options of any moneyness. This figure shows that a lower λ results in a higher implied volatility and a higher λ in a lower implied volatility. The figure also shows that the skew pattern is persistent for options across all moneyness.

Figure 4.9: Implied Volatility of American Put Option Under Heston Model

Figure 4.10 is the implied volatility of an American put options for $T = 1$; $S = 1$; $\theta = 0.46$; $\sigma = 2.78$; $\rho = -0.64$; $\lambda = -0.02$; $r = 0; 0.02$ and 0.03; $\kappa = 0.75$. From the figure, we see that r positively affects the implied volatility. When the options is out-of-the-money and at-the-money, the three curves are approximately parallel. However, when the option moves into slightly deeper in-the-money, a higher r has a more dramatic impact on raising the implied volatility, while the effect of a lower r is less pronounced. This explains why the curves start to diverge at the end of segment of the figure.
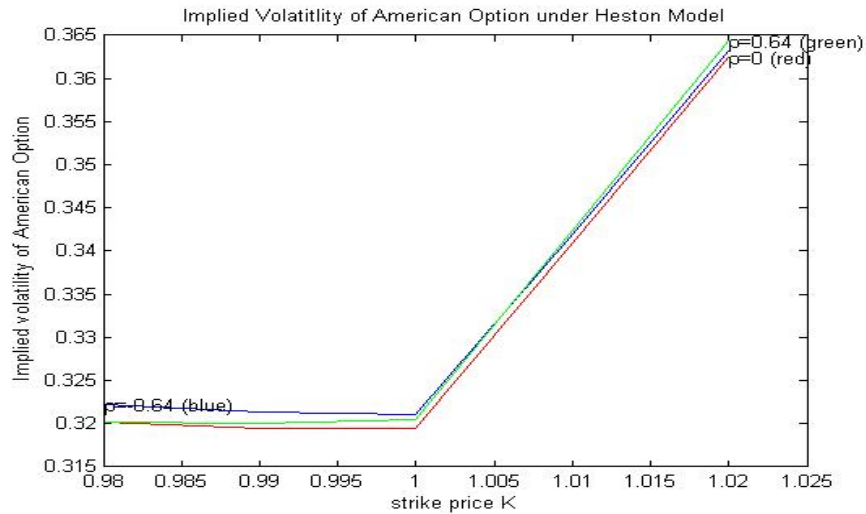
Figure 4.10: Implied Volatility of American Put Option Under Heston Model

Figure 4.11 is the implied volatility of an American put options for $T = 1$; $S = 1$; $\theta = 0.46$; $\sigma = 0.5$; 2.78; and 5; $\rho = -0.64$; $\lambda = -0.02$; $r = 0.02$; $\kappa = 0.75$. This figure shows that σ is negatively related to implied volatility. The lower the σ, the higher the implied volatility. The implied volatility increases when the option moves from out-of-the-money to in-the-money.
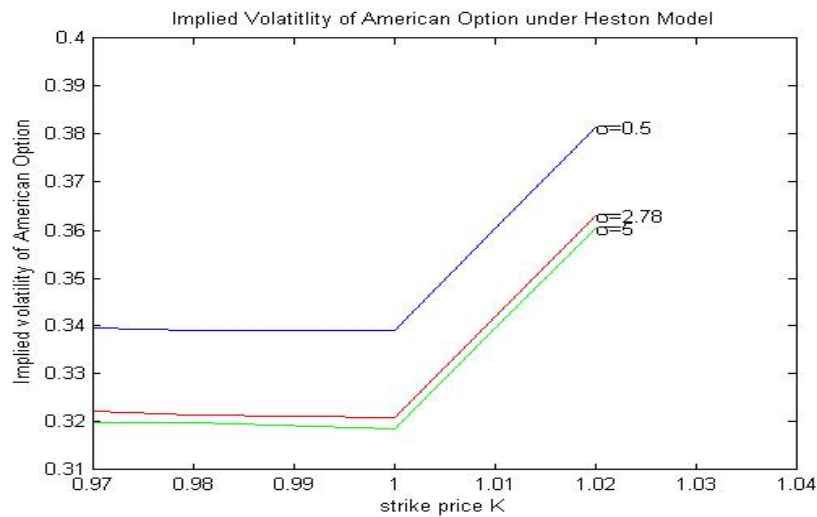
Figure 4.11: Implied Volatility of American Put Option Under Heston Model

4.2.2 A Comparison between American and European Options

A series of similar tests are applied to the European options to study and compare the volatility smiles for put options of the American and European styles. The method used to calculate the implied volatility of a European option is similar to that of an American option in the previous section. In order to form a comparative contrast, both options on the same underlying, with the same strike prices, maturities and parameters are tested, and the underlying is set at $S = 1$ and the strike price is set from 0.5 to 1.2 similar to that for the American options. In all of the figures in this section, trials are carried out by varying one parameter at a time.

Figure 4.12 is the implied volatility of American and European put options for $T = 1$; $S = 1$; $\theta = 0.46$; $\sigma = 2.78$; $\rho = -0.64$; $\lambda = -0.02$; $r = 0.02$; $\kappa = 0.75$ and $\kappa = 2$. It shows that with small κ, both American and European options show similar volatility smile pattern, however, as κ increases, the implied volatility of the in-the-money European option increases dramatically while that for the in-the-money American option show a persistent skew. Also, we notice that for the American put option, the implied volatility decreases when K is less than stock price S when $K < 1$ and then increases as K increases when $K > 1$. However, it suddenly slumps when $K > 1.2$. The reason is that too deep in- or out-of-the-money option prices are deterministic and do not follow the pricing model.
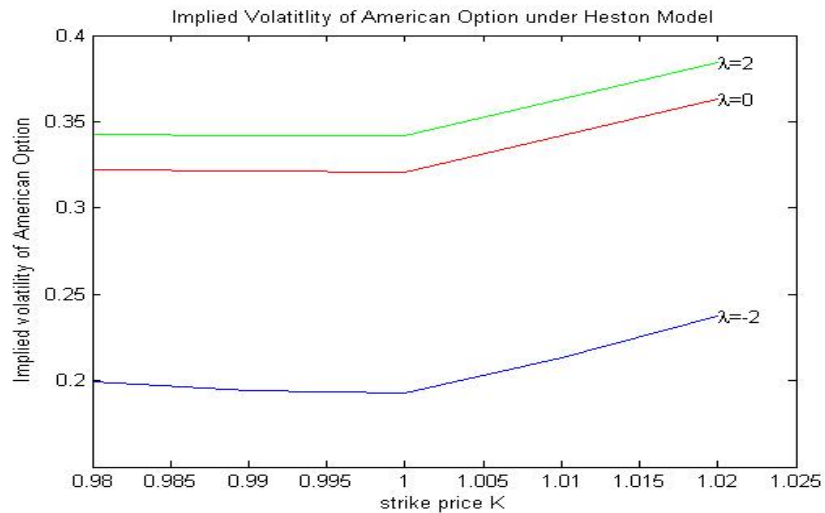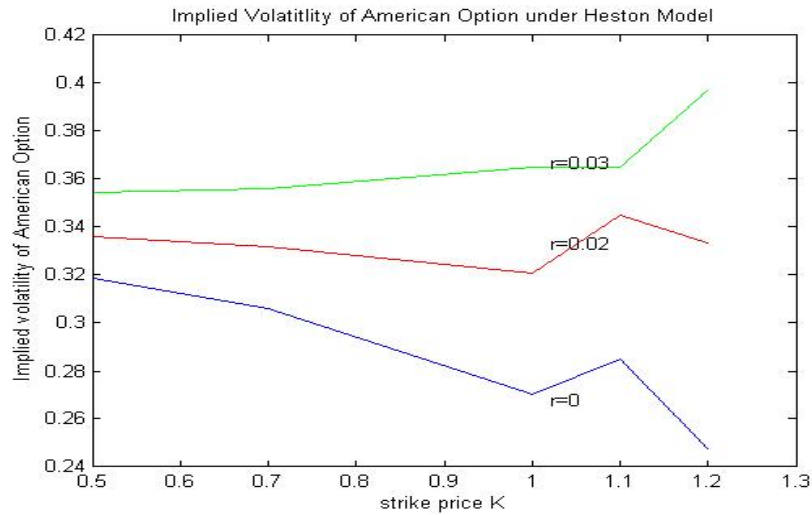

Figure 4.12: Implied Volatility of American vs European Put Option Under Heston Model

Figure 4.13 is the implied volatility of an American and European put options for $T = 1$;

$S = 1$; $\theta = 0.46$; and $\theta = 0.72$; $\sigma = 2.78$; $\rho = -0.64$; $\lambda = -0.02$; $r = 0.02$; $\kappa = 0.75$. It shows a similar pattern as in Figure 4.12. Both options show a comparable implied volatility pattern with a small θ. When θ becomes large, the in-the-money American options show a much sharper increase in implied volatility than that of in-the-money European options.

Figure 4.13: Implied Volatility of American vs European Put Option Under Heston Model

Figure 4.14 is the implied volatility of an American and European put options for $T = 1$; $S = 1$; $\theta = 0.46$; $\sigma = 2.78$; $\rho = -0.64$; and $\rho = 0.64$; $\lambda = -0.02$; $r = 0.02$; $\kappa = 0.75$. The two sets of curves are relatively close to each other and follow a similar tendency. Therefore, we can conclude that ρ has a comparable impact on the volatility smile of the European options, and the quantitative change of ρ has an equal effect on both options.

Figure 4.14: Implied Volatility of American vs European Put Option Under Heston Model

Figure 4.15 is the implied volatility of the American and European put options for $T = 1$; $S = 1$; $\theta = 0.46$; $\sigma = 2.78$; $\rho = -0.64$; $\lambda = -0.06$ and $\lambda = 0.06$; $r = 0.02$; $\kappa = 0.75$. It shows comparable implied volatility patterns with difference values of λ. Generally, In the figures, the in-the-money American put option has a higher implied volatility than the corresponding in-the-money European option.
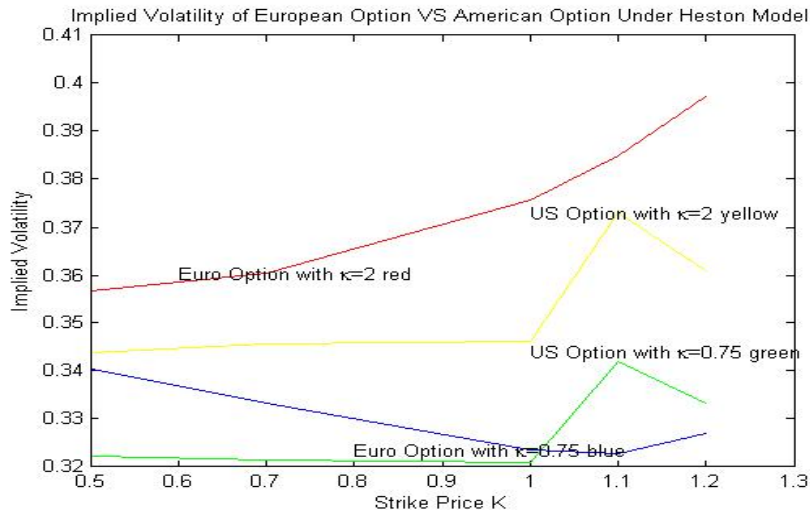

Figure 4.15: Implied Volatility of American vs European Put Option Under Heston Model

Figure 4.16 is the implied volatility of an American and European put options for $T = 1$; $S = 1$; $\theta = 0.46$; $\sigma = 2.78$; $\rho = -0.64$; $\lambda = -0.02$; $r = 0.02$; and $r = 0.04$; $\kappa = 0.75$. It depicts the effect of varying r. We observe that r has a uniform impact on the volatility smile pattern for both European and American options. For strike price $K > 1$, the in-the-money American options has a higher implied volatility than the otherwise similar European options.
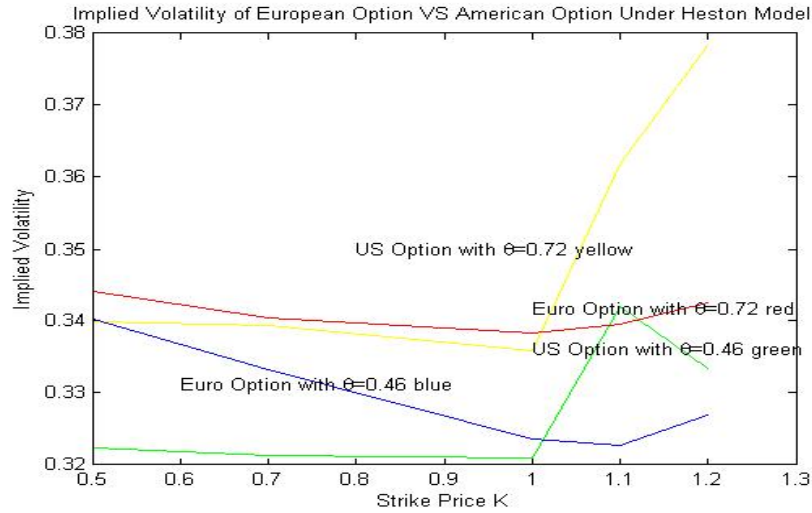
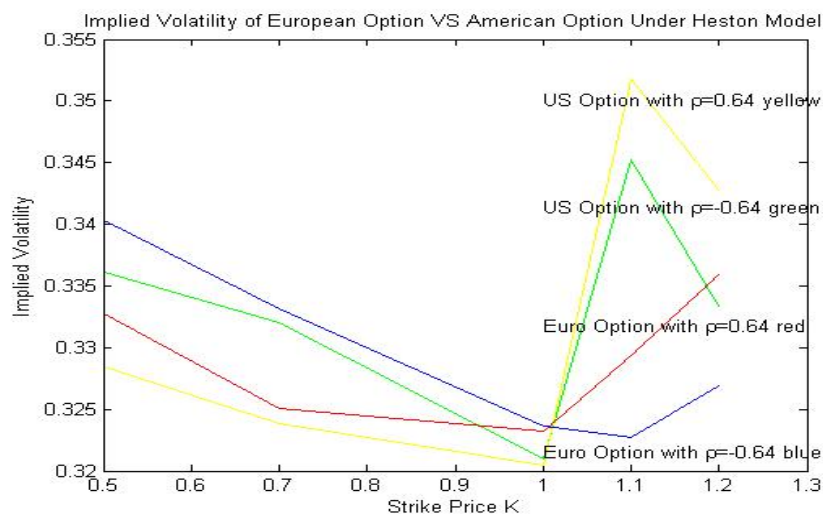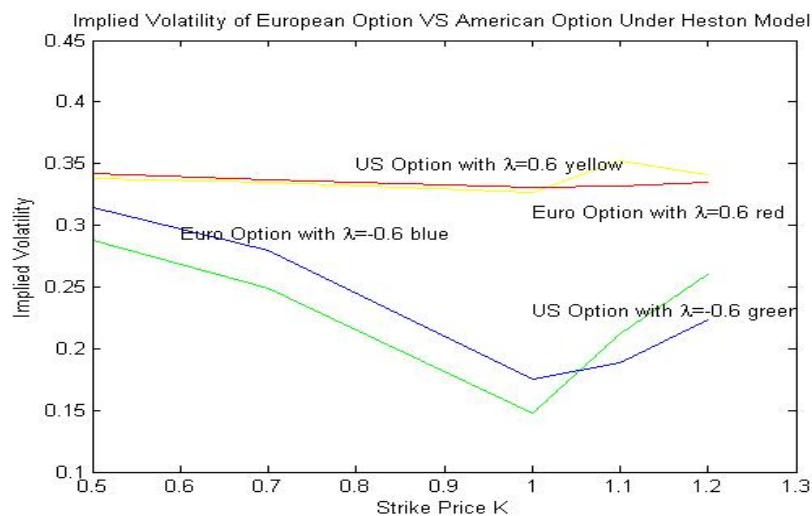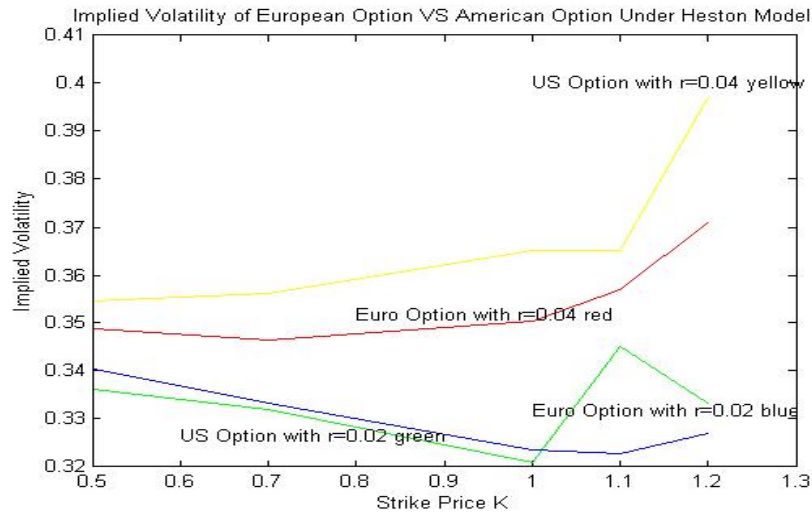

Figure 4.16: Implied Volatility of American vs European Put Option Under Heston Model

Figure 4.17 is the implied volatility of an American and European put options for $T = 1$; $S = 1$; $\theta = 0.46$; $\sigma = 1.4$; and $\sigma = 2.78$; $\rho = -0.64$; $\lambda = -0.02$; $r = 0.02$; $\kappa = 0.75$;.
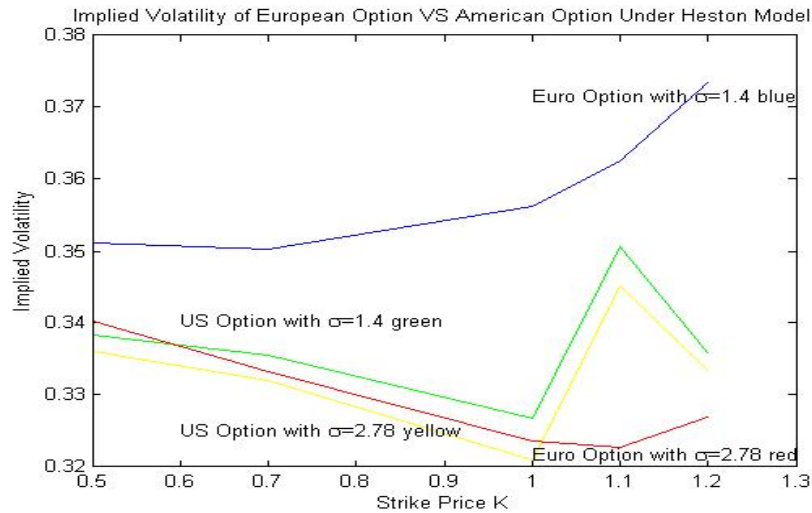
Figure 4.17: Implied Volatility of American vs European Put Option Under Heston Model

To sum up, volatility smiles generated by the Heston model on the European and American options share similar properties and follow similar patterns. The out-of-the-money American and European options have rather comparable implied volatilities, while the in-the-money European options having evidently higher implied volatility than the in-the-money American ones. The quantitative changes of the parameters have considerable effect on the value of implied volatilities, but this effect is common to both the European and American options.

Even though an American option usually has a value higher than its European counterpart, the implied volatility of an American option does not have to be always higher than that of a European one. Figures in this section show that when both options are in-the-money (underlying price < strike price), it is the European option that has a higher implied volatility. One possible explanation is that when both options are in-the-money, the American version can be exercised at any time and the profit is guaranteed. This results in lower investment risk and the trading would be less active than those at-the-money options or out-of-the-money options. In the real business, a tranquil market usually has a relatively lower volatility. Meanwhile, the European option is not guaranteed to expire in-the-money, thus the potential investment risk is higher and the trading is generally more active than its American counterpart. As such, we might expect a higher implied volatility for in-the-money European options than in-the-money American ones. On the other hand, when both options are out-of-the-money (underlying price > strike price), the figures show that the American options have a slightly higher implied volatility than the European

52

options. One possible reason is that the at-the-money and out-of-the-money options are traded most heavily in the market (more active than in-the-money options); based on this argument, an American option has a higher price thus a higher volatility while a European option a lower price and a lower volatility. The analysis above further indicates that the implied volatility is not only related to strike and maturity, but the moneyness (underlying and strike prices) as well; and a more sophisticated implied volatility model could include trading volume as a variable.

4.3 A Comparison between the Heston Model and the Black-Scholes Model

Comparison is done by analyzing option prices obtained from the Heston Model and the Black-Scholes model. Consider an American put option with strike=1 and 1 year to maturity Option prices, price-H and price-BS are calculated using the Heston model and the Black-Scholes model. The differences between each pair of option prices against the same underlying value are obtained as price-H-price-BS = Price Difference. Risk free rate are the same for both models, volatility in the Black-Scholes model is the implied volatility calculated in 4.2.1 with the same parameter values: $\kappa = 0.75$; $\theta = 0.46$; $\sigma = 2.78$; $\rho = -0.64$; $\lambda = -0.02$; $r = 0.02$. Figure 4.18 for price difference of an American put option between the Heston model and the Black-Scholes model, $T = 1$ year and strike price $K = 1$. Parameters in the Heston model: $\kappa = 0.75$; and 2; $\theta = 0.46$; $\sigma = 2.78$; $\rho = -0.64$; $\lambda = -0.02$; $r = 0.02$.

Figure 4.18: Price Difference between Prices from Heston Model and Black-Scholes Model

Figure 4.18 shows that the Heston model tends to underprice in-the-money options and overprice out-of-the-money options relative to the Black-Scholes model with comparable volatility. The price differences at the left and right ends are almost equal to zero as the option falls into the early exercise region when S is small and is deep out-of-the money when S is large. When the option is in-the-money but not in the early exercise region, the price difference, price H-price BS, is negative, which shows that the Heston price is smaller than the B-S price. Thus, the in-the-money option should be underpriced by the Heston model relative to the Black-Scholes model. However, when the option is out-of-the-money, the price difference is negative, indicating that this option is overpriced by the Heston model.

Furthermore, this pattern is increased with a decrease of κ, which is the mean reversion speed. When κ is reduced from 2 to 0.75, the price differences for both in-the-money and out-of-the-money options are roughly doubled. This figure also indicates that this pattern is more pronounced for the in-the-money and out-of-the-money options than the at-the-money options, as the two curves intersect at around where S is equal to the strike price.

Figure 4.19 for Price Difference of an American put option between the Heston model and the Black-Scholes model, T=1 year and strike=1. Parameters in the Heston model: $\kappa = 0.75$; $\theta = 0.46$ and 0.72; $\sigma = 2.78$; $\rho = -0.64$; $\lambda = -0.02$; $r = 0.02$.

Figure 4.19: Price Difference between Prices from Heston Model and Black-Scholes Model

Figure 4.19 shows a similar pattern as Figure 4.18. Compared with the Black-Scholes model, the Heston model tends to underprice in-the-money options and overprice out-of-the-money options. θ has a similar impact as κ on option prices. When θ is reduced from 0.92 to 0.46, the price differences for both the in- and out-of-the-money options are raised. This pattern is more notable for in- and out-of-the-money options than at the money options, as the two curves intersect at around where the underlying price is equal to strike price.

Figure 4.20 for Price Difference of an American put option between the Heston model and the Black-Scholes model, T=1 year and strike=1. Parameters in the Heston model: $\kappa = 0.75$; $\theta = 0.46$; $\sigma = 2.78$; $\rho = -0.64$; and 0.64; $\lambda = -0.02$; $r = 0.02$.
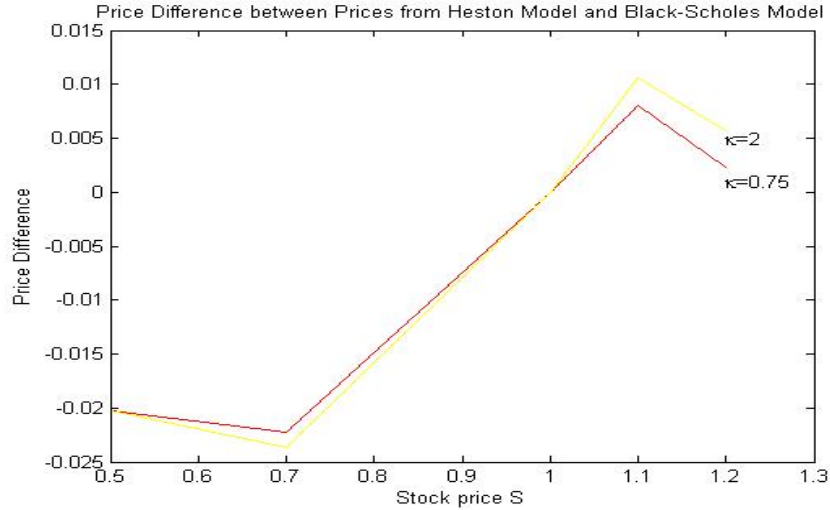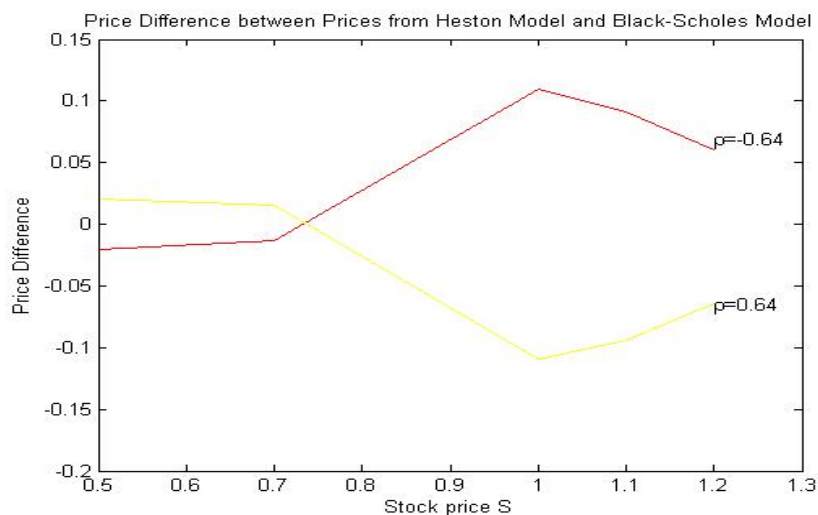
Figure 4.20: Price Difference between Prices from Heston Model and Black-Scholes Model

Figure 4.20 depicts two rather symmetric curves centered around where S equals to strike. It shows that Heston model tends to underprice in-the-money options and overprice out-of-the-money options when ρ is negative. When ρ is positive, the pattern is inverted, i.e. the Heston model overprices the in-the-money options and underprices the out-of-the-money options. When ρ is equal to -0.64, for the in-the-money options $S < 1$, the option price is overpriced by the Heston model; for the out-of-the-money options $S > 1$, the option price is underpriced by the Heston model. A negative ρ does exactly the opposite.

Figure 4.21 for Price Difference of an American put option between Heston model and the Black-Scholes model, $T = 1$ year and strike=1. Parameters in the Heston model: $\kappa = 0.75$; $\theta = 0.46$ $\sigma = 2.78$; $\rho = -0.64$; $\lambda = -0.6$; 0; and 0.6; $r = 0.02$.

56
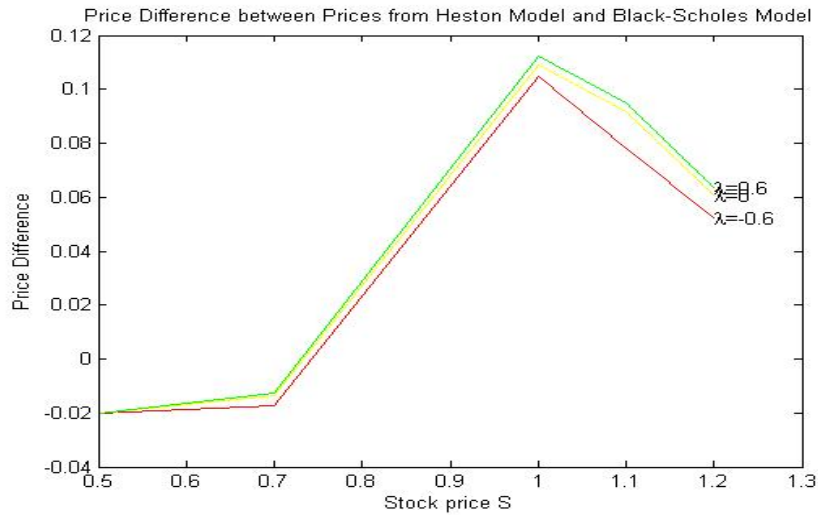
Figure 4.21: Price Difference between Prices from Heston Model and Black-Scholes Model

Figure 4.21 depicts a similar pattern Figures 4.18and 4.19. The three largely overlapping curves in Figure 4.21 indicates that the Heston model underprices the in-the-money options and overprices the out-of-the-money options relative to the Black-Scholes model with comparable volatility, and the change of λ, which is the market price of risk, has little effect on the pricing results of the Heston model.

Figure 4.22 for Price Difference of an American put option between the Heston model and the Black-Scholes model, T=1 year and strike=1. Parameters in the Heston model: $\kappa = 0.75$; $\theta = 0.46$; $\sigma = 1.4$; 2.78 and 5; $\rho = -0.64$; $\lambda = -0.02$; $r = 0.02$.
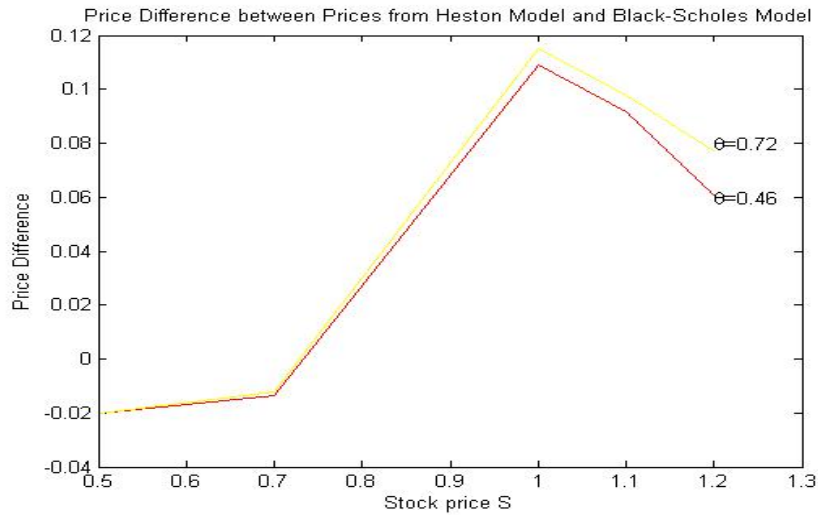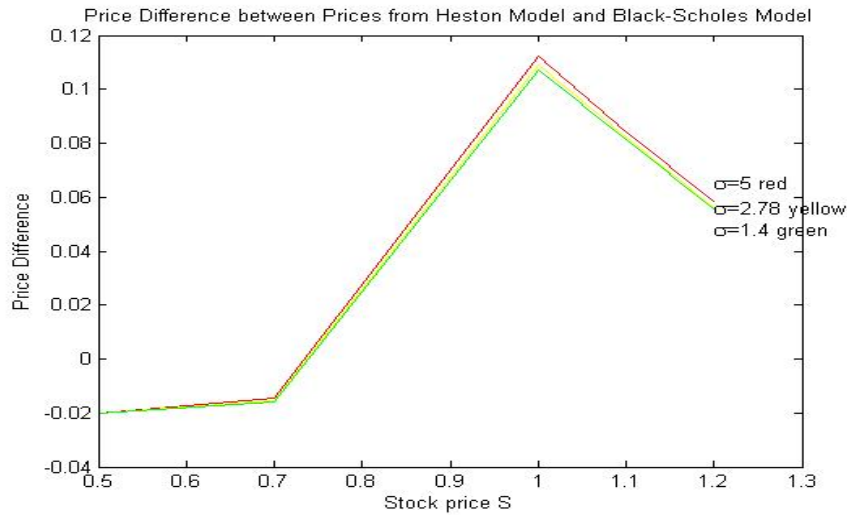
Figure 4.22: Price Difference between Prices from Heston Model and Black-Scholes Model

Figure 4.22 shows that the Heston model tends to underprice the in-the-money options and overprice the out-of-the-money options relative to the Black-Scholes model with comparable volatility. For an in-the-money option S < 1 not in the early exercise region, the Heston model tends to underprice this options with any value of σ . However, when S is greater than 1, the option goes out-of-the-money, and is overpriced for all values of σ . This impact is enhanced with a decrease of the value of σ. In this figure, with a decrease of σ from 5 to 1.4, the price gap increases gradually across all moneyness categories. The smallest $\sigma = 1.4$ results in the largest price gap, while the largest $\sigma = 5$ leads to the smallest price difference.

Figure 4.23 for Price Difference of an American put option between the Heston model and the Black-Scholes model, T=1 year and strike=1. Parameters in the Heston model: $\kappa = 0.75$; $\theta = 0.46$; $\sigma = 2.78$; $\rho = -0.64$; $\lambda = -0.02$; $r = 0$; 0.01; 0.02 and 0.2.

58
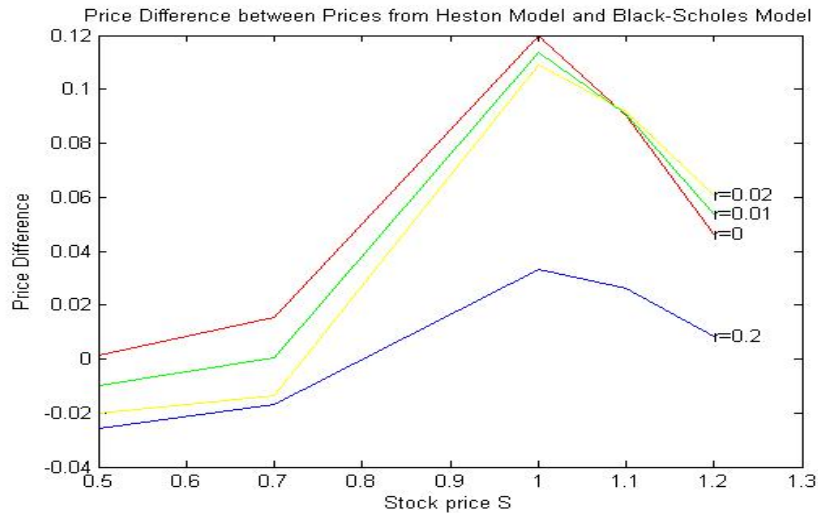
Figure 4.23: Price Difference between Prices from Heston Model and Black-Scholes Model

Figure 4.23 indicates that when the risk-free rate r is not too extreme, e.g., r does not drop to zero or increase above 0.2, the Heston model tends to underprice the in-the-money options and overprice the out-of-the-money options relative to the Black-Scholes model with comparable volatility. This pattern is shown by the two curves in the middle with $r = 0.01$ and $r = 0.02$. However, with a decrease of r, as shown by the first three curves, the pattern changes: the underpricing of in-the-money options diminishes gradually and the overpricing of out-of-the-money options augments steadily. When r decreases towards zero, the Heston model overprices options across all moneyness relative to the Black-Scholes model. The overpricing appears to be most pronounced for the out-of-the-money options. On the other hand, an increase of r shows the opposite effect. The last three curves show that with the increase of r, the underpricing of in-the-money option is more severe, and the overpricing of out-of-the-money option decreases gradually. When r reaches 20%, the Heston model seems to overprice the options of all moneyness relative to the B-S model. The overpricing effect is the most significant for the in-the-money options.

4.4 Calibration for Microsoft

4.4.1 Data Analysis

For the calibration exercise in this subsection, we choose the stock prices of Microsoft (MSFT) from January 3rd, 2009 to March 15th 2013 from Yahoo Finance. Figure 4.24 provides a time-series plot of the continuously compounded return of MSFT. We can observe a tendency of fluctuations of the return observations around the long-run mean level (zero in this case). This suggests that the data are likely to be weakly stationary. In addition, there is some evidence of persistence in the plot of squared return 4.25.

It is shown in Table 4.2 that the distribution of the daily returns is non-normal with negative skewness and pronounced excess kurtosis of 6.363896. This implies that the empirical distribution of the returns has thick tails. We also observe from Figure 4.26 that the upper tails for the QQ-plot turning upwards and the lower tails bending downwards from the straight line suggesting a heavy tailed distribution. The calculated Jarque-Bera test further confirms our assumption of nonnormality with a p-value less than 2.2e-16 which strongly rejects the null hypothesis of Normality assumption at an level of significance.

In the sample Auto Correlation Function (ACF) plot and the Partial Auto Correlation Function (PACF) plot of Figure 4.27 and Figure 4.28, we observe that the approximate 95% confidence bands include the sample autocorrelation coefficients at all lags. It indicates evidence of no serial correlation in the return observations. We further use the Box-Ljung Test for the joint insignificance of the sample autocorrelation coefficients for the first 10 lags to confirm our earlies assertion. The p-value turns out to be 0.1153. Hence, we can not reject the null hypothesis of no serial correlation in the return observations even at the 10 percent significance level.

Next, we test for the ARCH effect in the return data. An ARCH LM test has a p-value of 7.495e-08 which strongly rejects the null hypothesis of no ARCH effects against the ARCH process at any level of significance. Therefore, there is a significant ARCH effect in the return data suggesting that GARCH family models are needed to capture the volatility of the return over time.
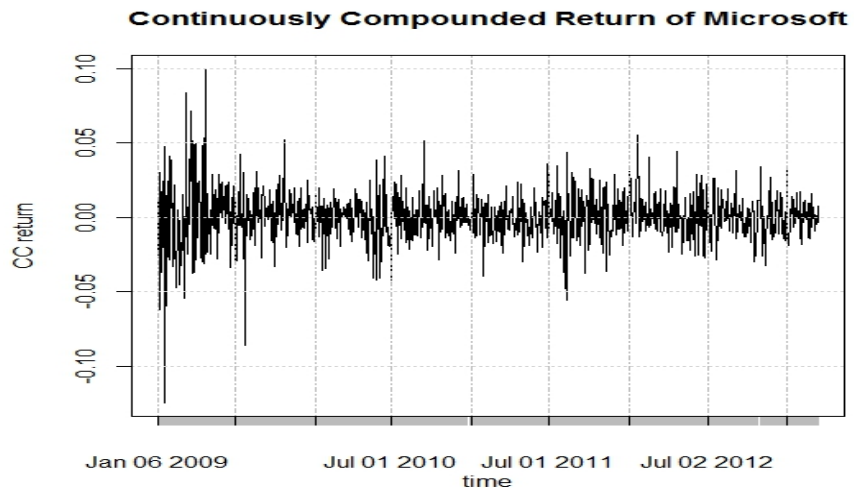
Figure 4.24: Time-series Plot of MSFT daily Returns
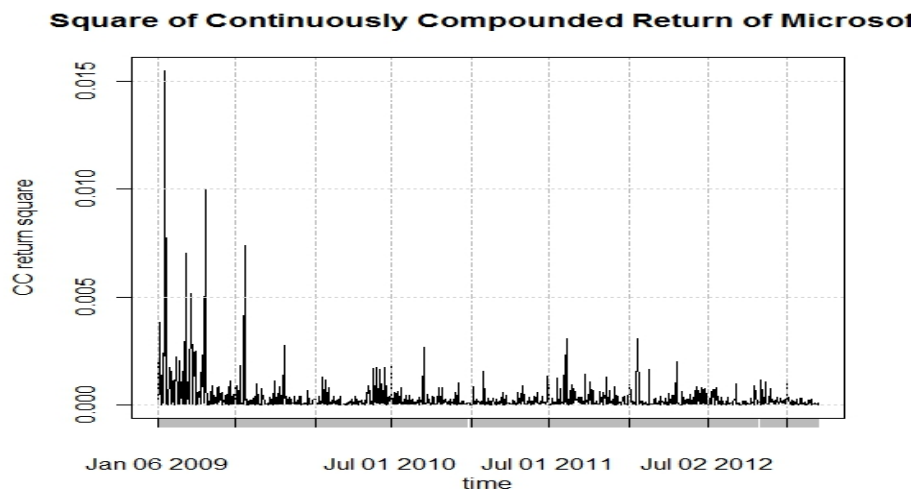
Figure 4.25: Time-series Plot of MSFT daily Squared Returns

μ	σ	skewness	kurtosis
0.0003967466	0.0164999	-0.1651116	9.363896

Table 4.2: Sample Moments of MSFT daily Returns
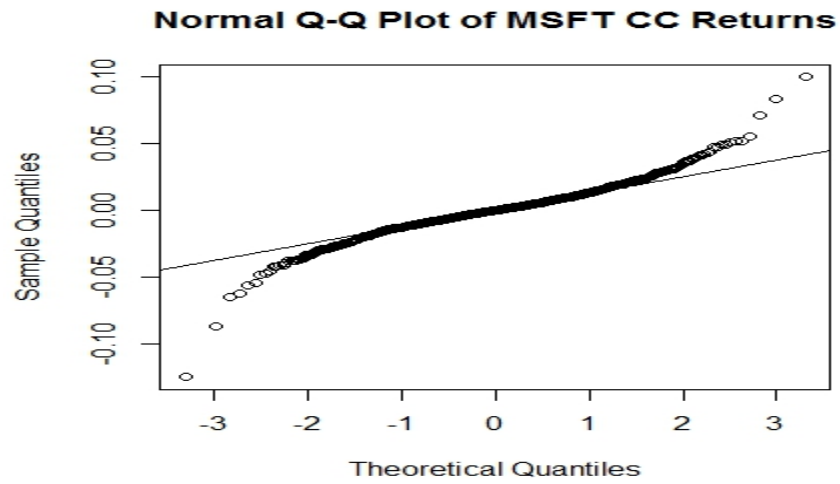
Figure 4.26: Q-Q plot of MSFT daily Returns
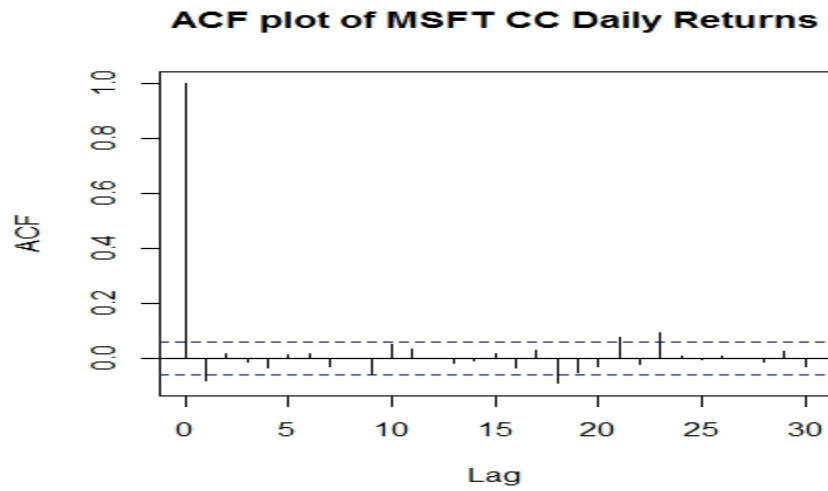
Figure 4.27: ACF plot of MSFT Daily Returns
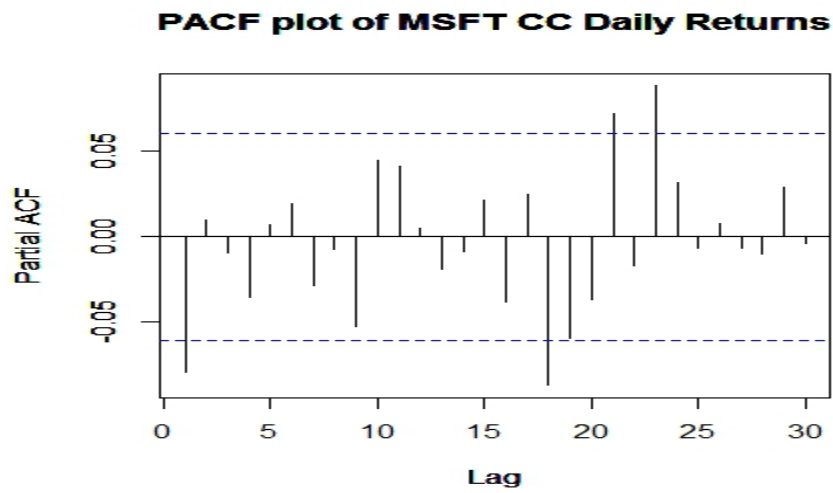
Figure 4.28: PACF plot of MSFT Daily Returns

Model	μ	ω	α_1	β_1	γ_1
	5.135743e-04	4.810741e-06	5.805665e-02	0.921167	NA
GARCH	[0.000431]	[0.000002]	[0.013470]	[0.018406]	NA
	(0.232905)	(0.017009)	(0.000016)	(0.000000)	NA
	0.000244	-0.116448	-0.040429	0.985538	0.124066
EGARCH	(0.000429)	(0.059818)	(0.014837)	(0.007188)	(0.025619)
	[0.569936]	[0.051571	[0.006433]	[0.000000]	[0.000001]
	0.000279	0.000004	0.052348	0.919315	0.430367
NAGARCH	[0.000439]	[0.000002]	[0.014184]	[0.021177]	[0.187995]
	(0.525246)	(0.042904)	(0.000224)	(0.000000)	(0.022065)
	0.000264	0.000349	0.083647	0.914883	0.270084
TGARCH	[0.000425]	[0.000136]	[0.013461]	[0.015854]	[0.120228]
	(0.533778)	(0.010439)	(0.000000)	(0.000000)	(0.024676)

Table 4.3: Maximum Likelihood Estimates of $\Psi = (a_1, \omega, \alpha_1, \beta_1, \gamma_1)$ for different auxiliary models

Models	GARCH	EGARCH	NAGARCH	TGARCH
Sign Bias	0.01663	0.07032	0.07740	0.1126
Negative Sign Bias	0.44668	0.41663	0.46875	0.3537
Positive Sign Bias	0.09153	0.08610	0.08829	0.1368
Joint Effect	0.10556	0.23917	0.25574	0.3374
likelihood	2932.584	2935.83	2935.455	2927.279
AIC	-5.5518	-5.5561	-5.5554	-5.5399
BIC	-5.5330	-5.5326	-5.5319	-5.5164

Table 4.4: All models above are of order (1,1) with the conditional mean of the return following ARMA(0,0) model

Table 4.11 shows the p-values from different tests, likelihood values, Akaike Information Criterion (AIC) values and Bayesian Information Criterion (BIC) values. Among all the models, we found that the EGARCH outperforms all other models since it has the largest likelihood value and smallest AIC value among all of the models. Also, the p-values for Sign bias test, Negative Sign Bias test, Positive Sign Bias test and Joint Effect test are smaller than 0.05 significance level.

Table 4.5: Summary Statistics about Microsoft Put Options 2013 February

| | Moneyness($x = S/K - 1$) | | | | | |
	Deep OTM Puts ($x < -0.05$)	OTM Puts ($-0.05 \leq x < -0.02$)	ATM Puts ($-0.02 \leq x < 0.02$)	ITM Puts ($0.02 \leq x < 0.05$)	Deep ITM Puts ($x \geq 0.05$)	All Puts
Average	0.64407	0.78885	1.09121	1.55312	2.93629	1.48229
StdDev	0.66696	0.70760	1.04555	0.80989	1.10201	2.00878
Total	166	109	194	104	163	1264

The summary statistics of Microsoft put option closing prices are reported for each moneyness-maturity groups. Moneyness is defined as $x = S/K - 1$, where S denotes the closing value of the dividend adjusted Microsoft and K denotes the exercise price of the option.

4.4.2 Calibration Result

Table 4.6: Summary Statistics about the Structure Parameters for February 1st, 2013 for Microsoft

κ	0.749131
θ	0.459467
σ	2.786400
ρ	-0.249205
λ	0.145000
V_t	0.062500

We employ 14 years of MSFT rolling daily stock price from January 2rd, 1999 to February 1st, 2013 to estimate the structure parameter of Heston model by indirect inference. The second step is to find the instantaneous variance V_t and volatility risk premium λ to minimize the distance between the market option prices from Chicago Board Options Exchange and the calibrated Heston model price for each day from February 1st to February 28th. Then, we incorporate the risk premium of volatility λ to transfer from the probability measure to the risk-neutral measure according to the equation (3.3). The table shows the estimated value of the mean-reverting speed, κ, long-term variance θ, the volatility of volatility, σ, the correlation coefficient between the asset return and its volatility, ρ, the risk premium, λ, and the instantaneous variance, V_t under the risk-neutral measure.
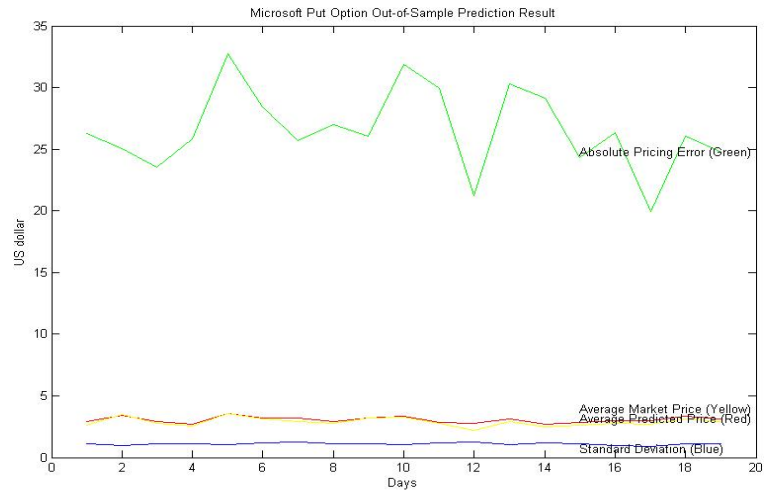
Figure 4.29: Microsoft Put Option Out-of-Sample Prediction Result

Table 4.7: Descriptive Statistics about Calibrated Prices and Market Prices for Microsoft

	Moneyness	Black-Scholes		Heston	
	$(S/K - 1)$	AbsError	stdev	AbsError	stdev
Deep OTM put	[0.05,∞]	0.64233	0.66727	0.62130	0.70567
OTM put	[0.02,0.05]	0.76541	0.70904	0.72089	0.73987
ATM put	[-0.02,0.02]	0.86671	1.05896	0.48913	1.00899
ITM put	[-0.05,-0.02]	0.65344	0.92762	0.58539	0.88472
Deep ITM put	[-∞,-0.05]	0.97475	0.76271	0.75672	1.01901
All put	[-∞,∞]	0.69289	0.83784	0.6349	0.7930

Table 4.8: Percentage Pricing Error

	B-S percentage pricing error (%)	Heston percentage pricing error (%)
Deep OTM Puts	-0.94273	0.20315
OTM Puts	0.35277	6.10070
ATM Puts	0.85923	0.12859
ITM Puts	-0.219551	-0.16512
Deep ITM Puts	-0.22189	-0.19401
All Puts	-0.35785	0.5967

We employ 14 years of MSFT rolling daily stock price from January 2rd, 1999 to February 1st, 2013 to estimate the structure parameter of Heston model by indirect inference. The second step is to find the instantaneous variance V_t and volatility risk premium λ to minimize the distance between the market option prices from Chicago Board Options Exchange and the calibrated Heston model price for each day from February 1st to February 28th. Then, we incorporate the risk premium of volatility λ to transfer from the probability measure to the risk-neutral measure according to the equation (3.3). For the Black-Scholes, we use the average of the implied volatility of all put options of the previous day. The reported absolute pricing error is the sample average of the absolute difference between the model price and the market price of each put in a given moneyness category. The reported percentage pricing error is the sample average of the model price minus the market price, divided by the market price. Moneyness is defined as the $S/K - 1$. OTM, ATM, and ITM represent out-of-the-money, at-the-money, and in-the-money options respectively.

We employ 14 years of MSFT rolling daily stock price from January 2rd, 1999 to February 1st, 2013 to estimate the structure parameter of Heston model by indirect inference. The second step is to find the instantaneous variance V_t and volatility risk premium λ to minimize the distance between the market option prices from Chicago Board Options Exchange

and the calibrated Heston model price for each day from February 1st to February 28th. Then, we incorporate the risk premium of volatility λ to transfer from the probability measure to the risk-neutral measure according to the equation (3.3). For the Black-Scholes model, we use the average of the implied volatility of all put options of the previous day.

For the sample Microsoft put option prices, only a selective number of strike prices are recorded. Extremely high or low values are omitted. By doing so, all the options chosen are around at-the-money. The reason is that the deep in- or out-of-the-money option prices are deterministic and do not follow the pricing model. These options would cause the failure of the model, thus resulting in unrealistic calibration results. Furthermore, the trading volume and computational results are also taken into account. Options having a sufficient trading volume are recorded as these options better reflect the true market movements. Extreme calibration results, such as zero interest rate, etc., are omitted and retain only reasonable outcomes to study the general pattern of the parameters. At last, we have 1264 American Style Microsoft index put option from February 1st, 2013 to February 28th, 2013.

We use absolute pricing error and percentage pricing error as the basis of assessing the performance of the calibrated model. The absolute pricing error is the sample average of the absolute difference between the model price and the market price of each put in a given moneyness category. The percentage pricing error is the sample average of the model price minus the market price, divided by the market price.

Table 4.7 reports the absolute pricing error of both Black-Scholes model and Heston model for each moneyness category. Overall, the Heston model outperforms the Black-Scholes model since the absolute pricing error for the Black-Scholes model is 0.69289 while the absolute pricing error for the Heston model is 0.6349. We notice that the magnitude of improvement is not very much notable. The Heston model performs best on at-the-money options with a smallest absolute pricing error of 0.48913. Generally, the deep in-the-money options, in-the-money options and at-the-money options are much better priced under the Heston model than the Black-Scholes model. Whereas, for the deep out-of-the-money case and out-of-the-money case, the Black-Scholes model has better performance than the Heston model.

Table 4.8 reports the percentage pricing errors of the Black-Scholes model and the Heston model. The result is consistent with Table 4.7. The Heston model are most accurate at estimating at-the-money option with a percentage pricing error of 0.12859. Meanwhile, the Heston model is inclined to perform better in the deep out-of-the-money options and out-of-the-money options than the the Black-Scholes model. Besides, we find that the Black-Scholes model tends to undervalue the deep out-of-the-money options, in-the-money

options and deep in-the-money options. This result supports the existence of volatility smile under the Black-Scholes model. Whereas, the Heston model is liable to overvalue the deep out-of-the-money options and the out-of-the-money options and underestimate the in-the-money options and the deep in-the-money options. It suggests that the Heston model generates a sneer smile.

4.5 Calibration of S&P 100

4.5.1 Data Analysis

Previously in Section 2, we have shown that the daily continuously compounded return of S&P 100 are likely to be weakly stationary, not normally distributed and serially correlated. To remove the serial correlation, we use an ARMA(p, q) Model. We end up with an ARMA(1,0). The p-value of the Box-Ljung test the residuals are generated by the ARMA(1,0) model is 0.08464, which is larger than 0.05. Thus there is no evidence of serial correlation left in the time series after fitting it with the ARMA (1,0) model.

μ	σ	skewness	kurtosis
0.0004406805	0.01235711	-0.2136038	6.748986

Table 4.9: Sample Moments of S&P100 Daily Returns

We conduct the ARCH LM-test to test for no ARCH effect in the return observations and the p-value turns out to be less than 2.2e-16 which rejects against an ARCH process the null hypothesis of no ARCH effects at any level of significance. Hence, we need a GARCH family model to capture the documented ARCH effects in the return data.

Model	μ	ω	α_1	β_1	γ_1
	-0.036541	0.000003	0.103034	0.878390	NA
GARCH	[0.033809]	[0.000001]	[0.0175520]	[0.017996]	NA
	(0.279782)	(0.001009)	(0.000000)	(0.000000)	NA
	-0.033433	-0.293074	-0.171785	0.966828	0.132993
EGARCH	(0.032156)	(0.060161)	(0.023256)	(0.006671)	(0.027104)
	[0.298478]	[0.000001]	[0.000000]	[0.000000]	[0.000001]
	-0.027784	0.000003	0.068202	0.759049	1.545379
NAGARCH	[0.032635]	[0.000001]	[0.014400]	[0.034699]	[0.269317]
	(0.394576)	(0.000000)	(0.000002)	(0.000000)	(0.000000)
	-0.043231	0.000368	0.094435	0.898817	1.000000
TGARCH	[0.041653]	[0.000066]	[6.4094]	[0.014053]	[0.169017]
	(0.29932)	(0.000000)	(0.00000)	(0.000000)	(0.000000)

Table 4.10: Estimates of $\Psi = (a_1, \omega, \alpha_1, \beta_1, \gamma_1)$ for different auxiliary models

Models	GARCH	EGARCH	NAGARCH	TGARCH
Sign Bias	0.11823	0.786264	0.72503	0.858485
Negative Sign Bias	0.07726	0.050141	0.03081	0.021909
Positive Sign Bias	0.01242	0.008088	0.01331	0.003281
Joint Effect	0.00136	0.010045	0.01125	0.002645
likelihood	3300.895	3336.67	3341.015	3337.214
AIC	-6.2500	-6.3160	-6.3242	-6.3170
BIC	-6.2312	-6.2924	-6.3007	-6.2935

Table 4.11: All of the models are of order (1,1) with the conditional mean of the return observations following the ARMA(1,0)

Among all of the models considered, we found that the NAGARCH(1,1) model is the best model since it has the largest the likelihood value and the smallest AIC value.

	Moneyness $(x = S/K - 1)$					
	Deep OTM Puts $(x < -0.05)$	OTM Puts $(-0.05 \leq x < -0.02)$	ATM Puts $(-0.02 \leq x < 0.02)$	ITM Puts $(0.02 \leq x < 0.05)$	Deep ITM Puts $(x \geq 0.05)$	All Puts
Average	2.12098	2.30965	7.54330	21.56667	41.40000	5.52196
StdDev	5.96152	2.42661	6.29493	4.58770	0.00000	9.50841
Total	230	215	306	30	1	988

Table 4.12: Summary Statistics about S&P 100 Put Options 2013 February

The summary statistics of S&P 100 put option closing prices are reported for each moneyness-maturity groups. Moneyness is defined as $x = S/K - 1$, where S denotes the closing value of the dividend adjusted Microsoft and K denotes the exercise price of the option.

4.5.2 Comparison of Pricing Results from the Black-Scholes Model and the Heston Model

Table 4.13: Summary Statistics about the Structure Parameters

κ	1.01569
θ	0.121881
σ	0.27777
ρ	0.408502
λ	0.0030
V_t	0.2990

We employ 14 years of S&P 100 rolling daily stock prices from January 2rd, 1999 to February 1st, 2013 to estimate the structure parameter of Heston model by indirect inference. The second step is to find the instantaneous variance V_t and volatility risk premium λ to minimize the distance between the market option prices from Chicago Board Options Exchange and the calibrated Heston model price for each day from February 1st to February 28th. Then, we incorporate the risk premium of volatility λ to transfer from the probability measure to the risk-neutral measure according to the equation (3.3). The table shows the estimated value of the the mean-reverting speed, κ, long-term variance, θ, the volatility of volatility, σ, the correlation coefficient between the asset return and its volatility, ρ, the risk premium, λ, and the instantaneous variance, V_t.
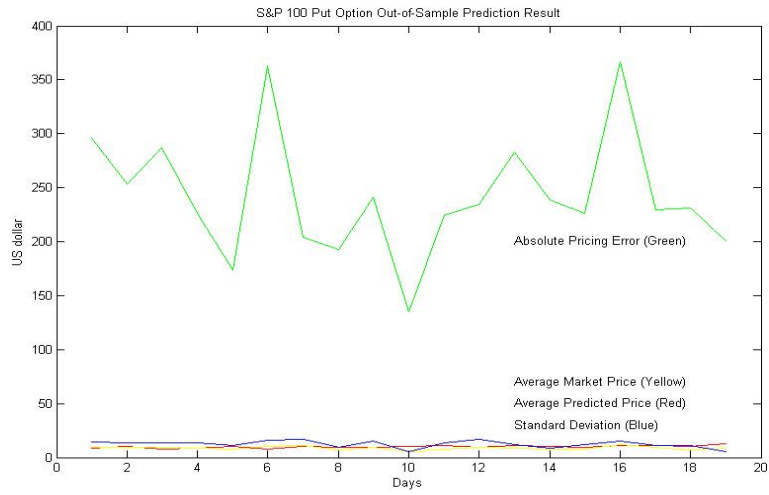
Figure 4.30: S&P 100 Put Option Out-of-Sample Prediction Result

Table 4.14: Absolute Pricing Error for S&P 100 Put Options

	Moneyness $(S/K-1)$	Black-Scholes		Heston	
		AbsError	stdev	AbsError	stdev
Deep OTM put	[0.05,∞]	2.07919	5.96551	2.04073	6.04812
OTM put	[0.02,0.05]	1.94634	2.49580	2.32024	3.10256
ATM put	[-0.02,0.02]	4.44581	6.50974	1.00974	5.79156
ITM put	[-0.05,-0.02]	4.98801	6.12835	2.20382	2.82369
Deep ITM put	[-∞,-0.05]	12.84873	0.00000	4.15000	0.00000
All put	[-∞,∞]	3.9415	9.01723	3.69139	9.03661

Table 4.15: Percentage Pricing Error

	B-S percentage pricing error (%)	Heston percentage pricing error (%)
Deep OTM Puts	-0.78503	2.23415
OTM Puts	3.80953	15.10427
ATM Puts	6.60467	0.02226
ITM Puts	-0.09146	-0.02277
Deep ITM Puts	-0.31036	-0.10024
All Puts	2.48643	5.47727

We employ 14 years of S&P 100 rolling daily stock price from January 2rd, 1999 to February 1st, 2013 to estimate the structure parameter of Heston model by indirect inference. The second step is to find the instantaneous variance V_t and volatility risk premium λ to minimize the distance between the market option prices from Chicago Board Options Exchange and the calibrated Heston model price for each day from February 1st to February 28th. Then, we incorporate the risk premium of volatility λ to transfer from the probability measure to the risk-neutral measure according to the equation (3.3). For the Black-Scholes model, we use the average of the implied volatility of all put options of the previous day. The reported absolute pricing error is the sample average of the absolute difference between the model price and the market price of each put in a given moneyness category. The reported percentage pricing error is the sample average of the model price minus the market price, divided by the market price. Moneyness is defined as the $S/K-1$. OTM, ATM, and ITM represent out-of-the-money, at-the-money, and in-the-money options respectively.

We employ 14 years of S&P 100 rolling daily stock price from January 2rd, 1999 to February 1st, 2013 to estimate the structure parameter of Heston model by indirect inference. The second step is to find the instantaneous variance V_t and volatility risk premium λ to

minimize the distance between the market option prices from Chicago Board Options Exchange and the calibrated Heston model price for each day from February 1st to February 28th. Then, we incorporate the risk premium of volatility λ to transfer from the probability measure to the risk-neutral measure according to the equation (3.3). For the Black-Scholes model, we use the average of the implied volatility of all put options of the previous day.

For the sample S&P 100 put option prices, only a selective number of strike prices are recorded. Extremely high or low values are omitted. By doing so, all the options chosen are around at-the-money. The reason is that deep in-the-money or out-of-the-money option prices are deterministic and do not follow the pricing model. These options would cause the failure of the model, thus resulting in unrealistic calibration results. Furthermore, the trading volume and computational results are also taken into account. Options having a sufficient trading volume are recorded as these options better reflect the true market movements. Extreme calibration results, such as zero interest rate, etc., are omitted and we decide to retain only reasonable outcomes to study the general pattern of the parameters. At last, we have 988 American Style S&P 100 index put option from February 1st, 2013 to February 28th, 2013.

We use the absolute pricing error and the percentage pricing error as the basis of assessing the performance of the calibrated model. The absolute pricing error is the sample average of the absolute difference between the model price and the market price of each put in a given moneyness category. The percentage pricing error is the sample average of the model price minus the market price, divided by the market price.

Table 4.14 reports the absolute pricing error of both the Black-Scholes model and the Heston model for each moneyness category. Overall, the Heston model outperforms the Black-Scholes since the absolute pricing error for the Black-Scholes model is 3.9415 while the absolute pricing error for the Heston model is 3.6914. We should notice that the magnitude of improvement is not very much notable. The Heston model performs best on at-the-money options with a smallest absolute pricing error of 1.00974. Generally, deep in-the-money options, in-the-money options and at-the-money options are much better priced under Heston model than the Black-Scholes model. Whereas, for the deep out-of-the-money case and out-of-the-money case, the Black-Scholes model has better performance than the Heston model.

Table 4.15 reports the percentage pricing error of the Black-Scholes model and the Heston model. The result is consistent with those reported in Table 4.14. The Heston model are most accurate at estimating at-the-money option with a percentage pricing error of 0.02226. Meanwhile, the Heston model is inclined to perform better in the deep out-of-the-money options and out-of-the-money options than the Black-Scholes. Besides,

we find that the Black-Scholes model tends to undervalue deep out-of-the-money options, in-the-money options and deep in-the-money options. This result supports the existence of volatility smile under the Black-Scholes model. Whereas, the Heston model is liable to overvalue deep out-of-the-money options and out-of-the-money options and underestimate the in-the-money options and deep in-the-money options. It suggests that the Heston model is likely to have a sneer smile.

Chapter 5

Conclusions

This thesis undertakes a systematic analysis of the pricing both the European option and the American option which is a path-dependence options, under the Black-Scholes model and the Heston (1993) stochastic volatility model. Under the Black-Scholes model, there is a closed form for European option. The derivation of the governing equation is identical for both European and American options, which are obtained by using Ito's lemma and the no arbitrage principle. However, a closed-form solution for the American options is not available and numerical computation needs to be adopted in order to implement the model. For the American option, we apply a Projected Successive Over-Relaxation Method. Under a risk-neutral measure, we use the risk free rate r as the drift term and either the historical volatility or the implied volatility can be used as the volatility. Under the Heston model, the European option has a semi-closed form while the American option is valued under the Alternating Implicit Method. We apply a two-step procedure to estimate the parameters of the Heston model under the risk-neutral measure on an American style option. In the first step, the indirect inference method is applied to estimate the model parameters by matching the NAGARCH model fitted by the historical time series of continuously compounded return and the simulated stock price from the Heston model. In the second step, we use the least squares principle to minimize the squared difference between market price and estimated prices so that the information from the market option price can be incorporated.

It is found that the American put option price will increase as we raise the value of the mean reverting speed κ, the long term variance θ and the instantaneous volatility V_t. While the option price is not sensitive to the market price of risk λ. As volatility of volatility σ, the risk free interest rate r and the stock price S grow, the American put option price will decrease.

Volatility smiles are analyzed to further examine the application of the Heston stochastic volatility model to the application of the Heston stochastic volatility model to the American put option. Different strike prices are used to calculate corresponding implied volatilities. when dealing with American options, the strike prices need to be chosen carefully to avoid too large or small values, as the over-high strike prices would bring the options to early exercise region while the over-low strike would make the option have little value. Either case would lead to the failure of the pricing model. The result from implied volatility of the American put option also supports the above conclusions. Implied volatility is found to be positively related with the mean reverting speed κ and the long term variance θ. For the market price of risk λ, if we use a very large value, we find that there is a positive relation between the option price and λ. However, we previously discover that the option price is not very sensitive to λ. A positive correlation ρ would cause the implied volatility to decrease from out-of-the-money to at-the-money and increase from at-the-money to in-the-money. It is the opposite way for a negative correlation, that is implied volatility increases from out-of-the-money and decreases from at-the-money to in-the-money. A larger risk free rate r would results in a higher implied volatility. The higher the volatility of volatility σ, the smaller the implied volatility is.

We observe implied volatilities of the European put option and the American put option under the Heston model display similar patterns. However, under different moneyness category, the implied volatilities varies slightly. The out-of-the-money American and European options show similar patterns of implied volatilities while the in-the-money American and European options show more distinctive differences. The implied volatility of a European option has a more sharply increasing slope than that of an American option.

Regarding the performance of both models, the Heston model is found to be most accurate at estimating at-the-money option. Also, the Heston model is inclined to perform better in deep out-of-the-money options and out-of-the-money options than the the Black-Scholes model. Besides, we find that the Black-Scholes model tends to undervalue deep out-of-the-money options, in-the-money options and deep in-the-money options. This result supports the existence of volatility smile under the Black-Scholes model. Whereas, the Heston model is liable to overvalue deep out-of-the-money options and out-of-the-money options and underestimate the in-the-money options and deep in-the-money options. It suggests that the Heston model generates a sneer smile.

References

[1] Back K. and Pliska S.R. On the fundamental theorem of asset pricing with an infinite state space. *Journal of Mathematical Economics*, 20:1–18, 1991.

[2] Black F. and Sholes M. The pricing of options and corporate liabilities. *The Journal of Political Economy*, 81(3), 1973.

[3] Bollerslev T. Generalized autoregressive conditional heteroskedasticity. *Journal of Business and Economic Statistics*, (14(2)):139–151, 1996.

[4] Cox J.C., Ingersoll J.E. and Ross S.A. A theory of the term structure of interest rates. *Econometrica*, 3:145–166, Mar. 1985.

[5] Cox J.C., Ingersoll J.E. and Ross S.A. The valuation of options for alternative stochastic processes. *Journal of Financial Economics*, 3:145–166, 1976.

[6] Engle R.F. and Ng V.K. Measuring and testing the impact of news on volatility. *Journal of Finance*, 48(5):1749–1778, 1993.

[7] Leoń A. Fiorentini G. and Rubio G. Estimation and empirical performance of heston's stochastic volatility model: the case of a thinly traded market. *Journal of Empirical Finance*, 9:225–255, 2002.

[8] Fjelland B. Thesis on application of the alternating direction implicit method. January 2012.

[9] Garman M.B. A general theory of asset valuation under diffusion state process. *Center for Research in Management Science*, (50), 1976.

[10] Gisige N. Risk-neutral probabilities explained. 2010. [SSRN: http://ssrn.com/abstract=1395390].

[11] Monfort A. Renault E. and Gouriéroux, C. Indirect inference. *Journal of Applied Econometrics*, (8):S85–S118, 1993.

[12] Harrison J.M. and Kreps D.M. Martingales and arbitrage in multiperiod securities markets. *Journal of Economic Theory*, 20:381–408, 1979.

[13] Harrison J.M. and Pliska S.R. Martingales and stochastic integrals in the theory of continuous trading. *Stochastic Processes and their Applications*, 11:215–260, 1981.

[14] Harrison J.M. and Pliska S.R. A stochastic calculus model of continuous trading: Complete markets. *Stochastic Processes and their Applications*, 15:313–316, 1983.

[15] Hentschel L. All in the family nesting symmetric and asymmetric garch models. *Journal of Financial Economics*, 39(1):71–104, 1995.

[16] Heston S.L. A closed-form solution for options with stochastic volatility with applications to bond and currency options. *The Review of Financial Studies*, 6(2):327–343, 1993.

[17] In't Hout K.J. and Foulon S. ADI finite difference scheme for option pricing in the heston model with correlation. *International Journal of Numerical Analysis and Modeling*, 7(2):303–320, 2002.

[18] Toivanen J. and Ikonen S. Efficient numerical methods for pricing american options under stochastic volatility. (B), 2005.

[19] Kainth I. *Foreign Exchange Option Pricing: A Practitioners Guide*. Wiley Finance, first edition, 2007.

[20] Taylor H.E. and Karlin S. *A Second Course in Stochastic Processes*. Academic Press, first edition, Apr. 1981.

[21] Kendall M. and Stuart A. The advanced theory of statistics. *Macmillan, New York*, 1, 1977.

[22] Nelson D.B. Conditional heteroskedasticity in asset returns: A new approach. *Econometrica*, 59:347–70, 1991.

[23] Gross P. Parameter estimation for black-scholes equation. 2006.

[24] Rachford H. H.and Peaceman D.W. The numerical solution of parabolic and elliptic differential equations. *J. Soc. Indust. Appl. Math.*, (3):28–41, 1955.

[25] Zhang J. and Shu, J.E. Pricing S&P 500 index options under stochastic volatility with the indirect inference method. *Journal of Derivatives Accounting*, 1(2):171–186, 2003.

[26] Marseken S. F. Surhone L. M. and Timpledon M. T. *Tridiagonal Matrix Algorithm*. Betascript Publishing, first edition, 2010.

[27] Howison S., Dewynne J. and Wilmott, P. *The Mathematics of Financial Derivatives: A Student Introduction*. The Press Syndicate of the University of Cambridge, third edition, 1995.

[28] Zakoian J.M. Threshold heteroskedastic models. *Journal of Economic Dynamics and Control*, 18(5):931–955, 1994.